

Holographical aspects of dyonic black holes: Massive gravity generalization

S. H. Hendi^{1,2*}, N. Riazi^{3†} and S. Panahiyan^{3‡}

¹ *Physics Department and Biruni Observatory, College of Sciences, Shiraz University, Shiraz 71454, Iran*

² *Research Institute for Astronomy and Astrophysics of Maragha (RIAAM), P.O. Box 55134-441, Maragha, Iran*

³ *Physics Department, Shahid Beheshti University, Tehran 19839, Iran*

The content of this paper includes studying holographical and thermodynamical aspects of dyonic black holes in the presence of massive gravity. For the first part of paper, thermodynamical properties of the bulk which includes black holes are studied and the main focus is on critical behavior. It will be shown that the existence of massive gravitons introduces remnant for temperature after evaporation of black holes, van der Waals phase transition for non-spherical black holes and etc. The consistency of different thermodynamical approaches toward critical behavior of the black holes is presented and the physical properties near the region of thermal instability are given. Next part of the paper studies holographical aspects of the boundary theory. Magnetization and susceptibility of the boundary are extracted and the conditions for having diamagnetic and paramagnetic behaviors are investigated. It will be shown that generalization to massive gravity results into the existence of diamagnetic/paramagnetic phases in phase structure of the hyperbolic and horizon flat of boundary conformal field theory.

I. INTRODUCTION

Considering different exact solutions for the massive objects, special attention is paid to the stringy black holes (see [1–3] for more details). These black holes enjoy the duality of electric/magnetic charges and possibly mass/dual mass [4]. In this regard, it was shown that two constants of a Taub-NUT system [5–10] can be interpreted as a gravitating dyon with both ordinary mass and its dual. In other words, the role of Nut charge is the mass duality, such as the duality between electric and magnetic charges in the $U(1)$ Maxwell theory [11, 12]. Dyonic black hole solutions and their interesting properties have been investigated in literature [13–33]. In this paper, we take into account a dyonic system in the context of massive gravity and obtain its exact black hole solutions.

It is well known that the usual general relativity can be understood as a unique theory of a massless spin-2 particle [34–37]. This theory is diffeomorphism invariant which implies a conserved stress-energy tensor. But in the massive case, there is no restriction to have a conserved source while its divergence can vanish for vanishing mass. The idea of massive spin-2 particle is a historical thought and the first academic works were done by Fierz and Pauli [38]. Since this theory suffers the vDVZ (van Dam-Veltman-Zakharov) discontinuity [39–41], its extension to nonlinear regimes was considered [42]. Nevertheless these nonlinear extensions of massive gravity lead to the presence of the Boulware-Deser ghost [43]. In order to solve this problem, various candidates have been suggested, among which we highlight the so-called DGP (Dvali-Gabadadze-Porrati) model [44–46], new massive gravity [47], bi-gravity [48] and dRGT (de Rham, Gabadadze and Tolley) theory [49–51]. In Ref. [52] the existence of ghost in dGRT massive gravity with Stückelberg fields was discussed and it was shown conclusively that this theory is ghost free. There are more attentions to dGRT massive gravity models and its extensions (dGRT-like models) [49–51, 53–57] which employ various models of reference metric for constructing the massive terms in the context of black holes. One of the interesting reference metrics was considered by Vegh in which the role of massive graviton can be regarded as lattice [58]. Such massive theory has been applied in various aspects of gravitation and astrophysics [59–64]. In addition, from the cosmological point of view, massive gravity has been considered before [48, 65–68]. It was also shown that the cosmological constant problem can be solved in the massive gravity context [66, 69–74]. Regarding the points mentioned above, the extension of massive gravity can open new theoretical avenues to have a deeper insight in various aspects of gravitating systems.

On the other hand, analyzing the effects of massive gravity on thermodynamics and phase transition of black holes is an interesting subject. Following the pioneering works of the Hawking and Bekenstein [75–77], one may regard the black objects as thermodynamical systems. In this regard, calculating conserved and thermodynamic quantities of the black holes, examining the validity of no-hair conjecture, and also the first law of thermodynamics are very

* email address: hendi@shirazu.ac.ir

† email address: n_riazi@sbu.ac.ir

‡ email address: sh.panahiyan@gmail.com

important. It is worthwhile to mention that investigation of the Hawking phase transition and thermal stability is an essential tool for considering a black hole as a real and viable thermodynamical system.

Recent progress in the black hole thermodynamics [78–81] and its relation to the AdS/CFT correspondence [82–88] imply the thermodynamical variability nature of the cosmological constant. The thermodynamical quantity related to cosmological constant was proposed to be pressure which is consistent with dimensional analysis [89]. This opened up the possibility of introduction of a van der Waals like behavior for the black holes. In this regard, the reentrant of the phase transition [90–93], existence of the triple point [94–96] and analogous heat engines [97–105] were investigated before. The van der Waals like behavior of the black holes based on different gravitational models and matter fields have been investigated in literature [106–140]. It was shown that depending on the gravity under consideration and employed matter fields, the critical behavior of the system may be modified and some conditions regarding the existence/absence of van der Waals like behavior will appear. Regarding the cosmological constant as a dynamical pressure also modifies the role of the mass of black holes into enthalpy of the system and first law of black hole thermodynamics. In this case, the phase space is told to be extended. For a beautiful review regarding the applications and implications of the extended phase space, we refer the reader to Ref. [141].

Our main motivation in this paper is exploring the effects of the graviton’s mass on thermodynamical structure of the dyonic black holes and holographical properties of the corresponding conformal field theory.

Now, we are ready to embark on our central task, namely, that of extending thermodynamic properties of dyonic black holes to the massive theory of gravitation. The outline of the present paper is as follows; First, the basic field equations governing Einstein massive dyonic gravity are given and black hole solutions are extracted. Then geometrical properties of the black holes are investigated and thermodynamical quantities are obtained. Next, some details regarding the enthalpy, temperature, heat capacity and free energy are given. In Sec. IV, the van der Waals like behavior, critical properties and conditions for presence/absence critical behavior of these black holes are investigated. Next, a comparative study regarding different phase diagrams is done and the connection between van der Waals like phase transitions and thermal stability of the solutions is discussed. Section VI, is devoted to study holographical aspects of conformal field theory. The magnetization properties are extracted and conditions regarding paramagnetism/ferromagnetism are extracted. The paper is concluded with some closing remarks.

II. BASIC EQUATIONS AND DYONIC BLACK HOLE SOLUTIONS

As we mentioned in the introduction, there are several approaches toward constructing a massive theory of the gravity. One of the most well-known theories was proposed by de Rham, Gabadadze and Tolley which is based on a reference metric. Employing a modified reference metric leads to construction of an interesting theory of massive gravity which is essentially dRGT-like. In general, the massive part of gravitational Lagrangian is given by

$$L_{massive} = m^2 \sum_i^4 c_i \mathcal{U}_i(g, \psi), \quad (1)$$

in which c_i ’s are arbitrary constants. Since we are interested in 4-dimensional solutions, \mathcal{U}_i are symmetric polynomials of the eigenvalues of the 4×4 matrix, $\mathcal{K}_\nu^\mu = \sqrt{g^{\mu\alpha}\psi_{\alpha\nu}}$ which can be written as follows:

$$\begin{aligned} \mathcal{U}_1 &= [\mathcal{K}], \\ \mathcal{U}_2 &= [\mathcal{K}]^2 - [\mathcal{K}^2], \\ \mathcal{U}_3 &= [\mathcal{K}]^3 - 3[\mathcal{K}][\mathcal{K}^2] + 2[\mathcal{K}^3], \\ \mathcal{U}_4 &= [\mathcal{K}]^4 - 6[\mathcal{K}^2][\mathcal{K}]^2 + 8[\mathcal{K}^3][\mathcal{K}] + 3[\mathcal{K}^2]^2 - 6[\mathcal{K}^4]. \end{aligned} \quad (2)$$

Here, $\psi_{\alpha\nu}$ and $g^{\mu\alpha}$ are, respectively, the reference metric and line element of spacetime. It is worthwhile to mention that depending on the choices of reference metric, the functional form of \mathcal{U}_i ’s may be modified.

The phrase of dyonic comes from specific consideration of gauge field theory. Here, in order to obtain topological dyonic solutions, we consider electromagnetic gauge potential one-form with the following explicit form

$$A = \left(\frac{q_E}{r_+} - \frac{q_M}{r} \right) dt + q_M \Upsilon d\varphi, \quad (3)$$

where q_E and q_M are two constants which are related to the electric and magnetic charges, respectively. Depending on choices of topology, Υ can be considered as

$$\Upsilon = \begin{cases} \cos \theta & k = 1 \\ \theta & k = 0 \\ \cosh \theta & k = -1 \end{cases}, \quad (4)$$

where $k = 1, 0$ and -1 represent spherical, flat and hyperbolic horizons of dyonic black holes, respectively. Based on Eq. (3), one finds $A_t(r = r_h) = 0$ which is a necessary condition for regularity at the horizon, since $g_{tt} \rightarrow 0$ when $r \rightarrow r_h$.

The 4-dimensional action governing Einstein massive dyonic black holes in the presence of the Maxwell electromagnetic field is given by

$$\mathcal{I} = -\frac{1}{16\pi G_4} \int d^4x \sqrt{-g} \left[\mathcal{R} - 2\Lambda - F^{\mu\nu} F_{\mu\nu} + m^2 \sum_i^4 c_i \mathcal{U}_i(g, \psi) \right], \quad (5)$$

where \mathcal{R} is the scalar curvature, $\Lambda = -\frac{3}{l^2}$ is the negative cosmological constant and G_4 is the Newton constant in 4 dimension. Also, $F_{\mu\nu} = \partial_\mu A_\nu - \partial_\nu A_\mu$ is the electromagnetic field tensor and A_μ is the gauge potential.

Using the variational principle with the action of Einstein–Maxwell massive gravity (5), it is a matter of calculation to show that field equations are given by

$$G_{\mu\nu} + \Lambda g_{\mu\nu} - \left[2F_{\mu\lambda} F_\nu^\lambda - \frac{1}{2} g_{\mu\nu} F^{\sigma\rho} F_{\sigma\rho} \right] + m^2 \chi_{\mu\nu} = 0, \quad (6)$$

$$\partial_\mu (\sqrt{-g} F^{\mu\nu}) = 0, \quad (7)$$

where in the above equation, $G_{\mu\nu}$ is the Einstein tensor and $\chi_{\mu\nu}$ is the contribution of massive terms in the field equation, which is

$$\begin{aligned} \chi_{\mu\nu} = & -\frac{c_1}{2} (\mathcal{U}_1 g_{\mu\nu} - \mathcal{K}_{\mu\nu}) - \frac{c_2}{2} (\mathcal{U}_2 g_{\mu\nu} - 2\mathcal{U}_1 \mathcal{K}_{\mu\nu} + 2\mathcal{K}_{\mu\nu}^2) - \frac{c_3}{2} (\mathcal{U}_3 g_{\mu\nu} - 3\mathcal{U}_2 \mathcal{K}_{\mu\nu} + \\ & 6\mathcal{U}_1 \mathcal{K}_{\mu\nu}^2 - 6\mathcal{K}_{\mu\nu}^3) - \frac{c_4}{2} (\mathcal{U}_4 g_{\mu\nu} - 4\mathcal{U}_3 \mathcal{K}_{\mu\nu} + 12\mathcal{U}_2 \mathcal{K}_{\mu\nu}^2 - 24\mathcal{U}_1 \mathcal{K}_{\mu\nu}^3 + 24\mathcal{K}_{\mu\nu}^4). \end{aligned} \quad (8)$$

Here, our main motivation is studying thermodynamical and holographical aspects of topological massive dyonic black holes. Therefore, we consider the metric of 4-dimensional spacetime as

$$ds^2 = -f(r) dt^2 + \frac{dr^2}{f(r)} + r^2 d\Omega^2, \quad (9)$$

in which

$$d\Omega^2 = \begin{cases} d\theta^2 + \sin^2 \theta d\varphi^2 & k = 1 \\ d\theta^2 + d\varphi^2 & k = 0 \\ d\theta^2 + \sinh^2 \theta d\varphi^2 & k = -1 \end{cases}. \quad (10)$$

As for the reference metric, we employ the following ansatz which was first introduced by Vegh [58] and then was generalized by Cai, et al. in Ref. [142]

$$\psi_{\mu\nu} = \frac{c^2}{r^2} g_{\mu\nu} |_{t=cte, r=cte}, \quad (11)$$

where c is a positive constant. By using reference (11) and spacetime (9) metrics with Eq. (2), one can obtain \mathcal{U}_i in the following forms

$$\mathcal{U}_1 = \frac{2c}{r}, \quad \mathcal{U}_2 = \frac{2c^2}{r^2}, \quad \mathcal{U}_3 = 0, \quad \mathcal{U}_4 = 0. \quad (12)$$

Using the obtained \mathcal{U}_i 's with metric (9) and Eqs. (6) and (7), one can extract the metric function, $\psi(r)$, as

$$f(r) = k + \frac{r^2}{l^2} - \frac{2m_0}{r} + \frac{q_E^2 + q_M^2}{r^2} + m^2 \left(\frac{cc_1}{2} r + c^2 c_2 \right), \quad (13)$$

where m_0 is an integration constant which is related to the total mass of massive dyonic black holes. In the absence of massive parameter ($m = 0$), obtained solutions (13) reduce to the usual topological dyonic black holes [143]

$$f(r) = k + \frac{r^2}{l^2} - \frac{2m_0}{r} + \frac{q_E^2 + q_M^2}{r^2}. \quad (14)$$

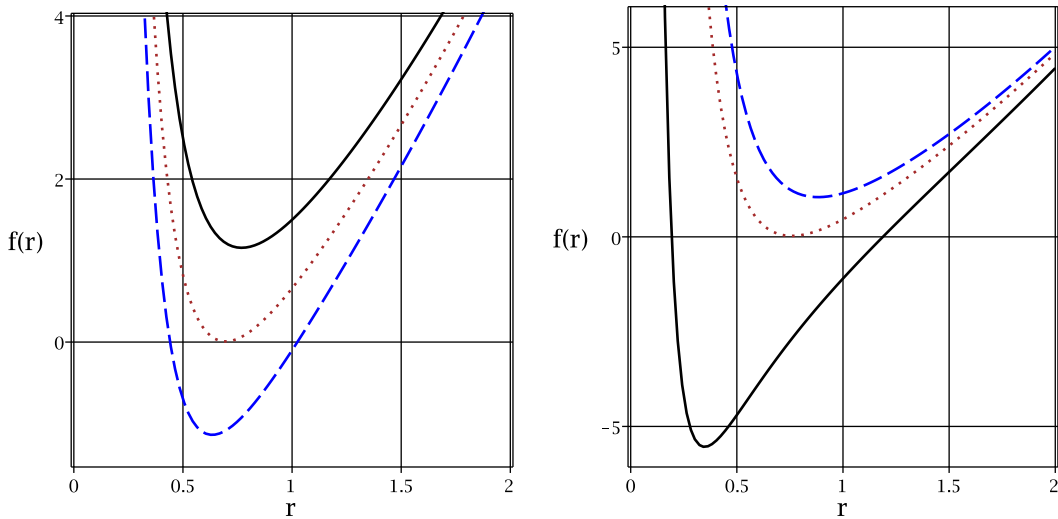


FIG. 1: $\psi(r)$ versus r for $b = 1$, $Q_E = 1$, $m = 1$, $c = c_1 = c_2 = 1$ and $k = 1$;
Left diagram: for $q_M = 1$, $m_0 = 2$ (continuous line), $m_0 = 2.42$ (dotted line) and $m_0 = 2.8$ (dashed line).
Right diagram: for $m_0 = 2.8$, $q_M = 0$ (continuous line), $q_M = 1.25$ (dotted line) and $q_M = 1.5$ (dashed line).

The existence of singularity and horizon indicates that our solutions can be intrinsically black holes. The presence of singularity could be investigated by studying curvature scalars for which we choose the Ricci and Kretschmann scalars. It is a matter of calculation to show that for these black holes the mentioned two scalars are

$$R = 2 \frac{k-1}{r^2} - \frac{c(3rc_1 + 2cc_2)m^2}{r^2} - \frac{12}{l^2},$$

$$R_{\alpha\beta\gamma\delta}R^{\alpha\beta\gamma\delta} = \frac{24}{l^4} + \frac{8(k-1) + 4c(3rc_1 + 2cc_2)m^2}{r^2l^2} + \frac{4(k-1)^2}{r^4} + \frac{8(k-1)(q_E^2 + q_M^2)}{r^6} + \frac{56(q_E^2 + q_M^2)^2}{r^8}$$

$$- 16 \left[(k-1) + \frac{6(q_E^2 + q_M^2)}{r^2} \right] \frac{m_0}{r^5} + \frac{48m_0^2}{r^6} + 2c^2 \left[(rc_1 + cc_2)^2 + c^2c_2^2 \right] \frac{m^4}{r^4}$$

$$- \left[\frac{4c(rc_1 - 2cc_2)(q_E^2 + q_M^2)}{r^2} + \frac{16c^2c_2m_0}{r} - 4c(k-1)(rc_1 + 2cc_2) \right] \frac{m^2}{r^4},$$

which confirm the existence of essential singularity at the origin since

$$\lim_{r \rightarrow 0} R \rightarrow \infty, \quad (15)$$

$$\lim_{r \rightarrow 0} R_{\alpha\beta\gamma\delta}R^{\alpha\beta\gamma\delta} \rightarrow \infty. \quad (16)$$

The Ricci and Kretschmann scalars are $\frac{-12}{l^2}$ and $\frac{24}{l^4}$ for $r \rightarrow \infty$. Considering $l^2 = \frac{\pm 3}{\Lambda}$, the asymptotical behavior of these solutions is (a)dS for $\Lambda < 0$ ($\Lambda > 0$).

Now, we focus on the existence of horizon. Due to complexity of the obtained metric function, it is not possible to study its roots (which are the horizons) analytically. Therefore, we employ numerical evaluation and plot some diagrams for finding the possible roots for the metric function (Figs. 1 and 2).

Evidently, the existence of horizon and their numbers are highly sensitive to values of the massive parameters. By suitable choices of different parameters, these black holes may have Reissner-Nordström like behavior (Fig. 1). Meaning, that they may have: two horizons, one extreme horizon or no horizon. On the other hand, for another set of values for different parameters, the Reissner-Nordström like behavior will be modified and existence of more than two horizons will be observed (see Fig. 2). The geometrical structure of the black holes depends on the number and type of horizons. In other words, it is possible to have usual horizon for outer horizon or an extreme one depending on choices of massive parameters. Since the existence of multi horizons was discussed before [61], we ignore it and concentrate on thermodynamic behavior. In addition, it is worthwhile to mention that the metric function with no real positive root results into the absence of horizon covering the singularity. This case is known as naked singularity and is not of interest in this paper.

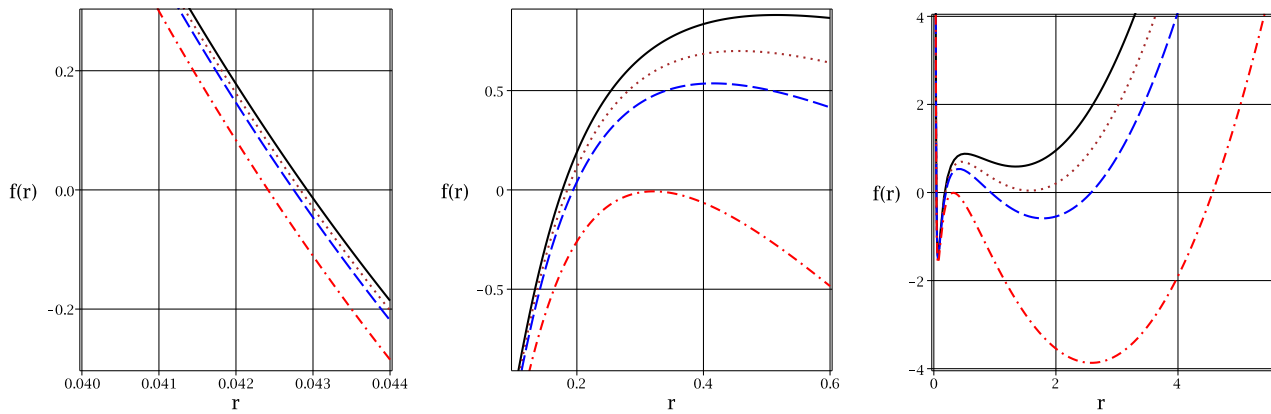


FIG. 2: **For different scales:** $\psi(r)$ versus r for $b = 1$, $q_E = q_M = 0.1$, $m = 0.3$, $c = 3$, $c_2 = 1$ and $k = 1$; For $c_1 = -8$ (continuous line), $c_1 = -9$ (dotted line), $c_1 = -10$ (dashed line) and $c_1 = -14$ (dashed-dotted line).

III. THERMODYNAMICAL QUANTITIES

Our next step for studying holographical aspects of massive dyonic black holes is obtaining thermodynamical quantities. The Hawking temperature could be obtained by employing the concept of surface gravity. Using this concept, the Hawking temperature on the outer horizon of these black holes (r_+) is given by

$$T = \frac{1}{4\pi} \left[\frac{k}{r_+} + \frac{3r_+}{l^2} - \frac{q_E^2 + q_M^2}{r_+^3} + m^2 \left(cc_1 + \frac{c^2 c_2}{r_+} \right) \right]. \quad (17)$$

The obtained black hole solutions in bulk are asymptotically *AdS* which are related to a *CFT* theory living on the boundary of bulk. The electromagnetic field of bulk is dual to global $U(1)$ current operator J_μ . It is a matter of calculation to show that the conserved global charge of the *CFT* related to this current is given by [143]

$$\langle J^t \rangle = \frac{q_E}{16\pi G_4}, \quad (18)$$

which by using the holographic dictionary, one can obtain [143]

$$\langle J^t \rangle = \frac{\sqrt{2} N^{\frac{3}{2}}}{24\pi l^2} q_E, \quad (19)$$

in which N is the degree of gauge group in *CFT*. Studying asymptotic value of the bulk field strength (from Eq. (3)) shows that the boundary *CFT* has a magnetic field strength

$$B = \frac{q_M}{l^2}, \quad (20)$$

which may be employed to study holographical aspects of the boundary theory.

The total mass of these black holes could be obtained by using Arnowitt-Deser-Misner approach or on shell action method [143]. The total mass is given by

$$M = \frac{r_+}{2} \left[k + \frac{r_+^2}{l^2} + \frac{q_E^2 + q_M^2}{r_+^2} + m^2 \left(\frac{cc_1}{2} r_+ + c^2 c_2 \right) \right]. \quad (21)$$

Recent progresses in studying thermodynamical structure of the black holes suggest that the cosmological constant plays the role of a thermodynamical variable. In other words, this quantity is a variable which can be interpreted as the thermodynamical pressure. The relation between the cosmological constant and pressure for the Einstein black holes can be written as

$$P = -\frac{\Lambda}{8\pi} = \frac{3}{8\pi l^2}. \quad (22)$$

It is worthwhile to mention that generalization to scalar-tensor theories modifies the mentioned relation between thermodynamical pressure and cosmological constant (22), while the massive gravity does not have any effect on this

relation. It should be pointed out that it is possible to construct massive theory of gravity using scalar tensor theories [144, 145]. In this case, the relation between pressure and cosmological constant could be affected by massive nature of the gravity. Replacing l with its corresponding pressure in total mass, one can obtain enthalpy for these black holes

$$H = \frac{4\pi P}{3} r_+^3 + \frac{r_+}{2} \left[k + \frac{q_E^2 + q_M^2}{r_+^2} + m^2 \left(\frac{cc_1}{2} r_+ + c^2 c_2 \right) \right]. \quad (23)$$

The electric potential for our solution is given by

$$\Phi_E = \frac{q_E}{r_+}. \quad (24)$$

Hereon, we are interested in doing our study in an ensemble in which its asymptotic value of A_t (electric potential) is constant. Therefore, we will replace q_E with its corresponding electric potential, Φ_E , in thermodynamical quantities. Such case corresponds to fixing the chemical potential in *CFT*. The mechanism here is to consider the A_t component of the electromagnetic potential vector as a fixed value on the horizon (with respect to infinity) and replace all the corresponding quantities related to electric field with the electric potential.

Using enthalpy, we can extract other thermodynamical quantities with the following forms

$$V = \frac{\partial H}{\partial P} = \frac{4\pi}{3} r_+^3, \quad (25)$$

$$q_E = \frac{\partial H}{\partial \Phi_E} = \frac{r_+ \Phi_E}{G_4}, \quad (26)$$

$$\Phi_M = \frac{\partial H}{\partial q_M} = \frac{q_M}{G_4 r_+}, \quad (27)$$

$$S = \frac{\partial H}{\partial T} = \frac{1}{4G_4} 4\pi r_+^2. \quad (28)$$

Here, Φ_M represents the intensive variable related to magnetic charge.

The free energy can be written as

$$W = H - TS - \Phi_E q_E, \quad (29)$$

where by using the obtained thermodynamical quantities, one can extract the free energy of massive dyonic black hole in the following form

$$W = -\frac{2\pi P}{3} r_+^3 + \frac{r_+}{4} \left[k + \frac{3q_M^2}{r_+^2} - \Phi_E^2 + m^2 c^2 c_2 \right]. \quad (30)$$

Now, we are in a position to study thermodynamic and holographic structures of the massive dyonic black holes.

A. Mass/Enthalpy

The mass of black holes is the same as internal energy in usual thermodynamics whereas by employing the relation between the cosmological constant and thermodynamical pressure, it will be interpreted as the enthalpy. Let us focus on it being enthalpy. First of all, the horizon radius has polynomial-like behavior which indicates that there exists an extremum for the enthalpy. The dominant term for small black holes is the q_M term, whereas, for large black holes, the P term is dominant. Since these parameters are positive valued, it is safe to say that the extremum for these black holes is actually a minimum.

Due to the nature of P , Φ_E , q_M , m and c , these parameters are positive and they have positive contributions to the values of enthalpy. On the other hand, c_1 , c_2 and k could be negative or positive. Therefore, they could either contribute negatively or positively to the enthalpy. If we consider the latter parameters to be positive, the enthalpy will be always positive without any root. But, if we take them to be negative valued, it may be possible to obtain one or two roots for the enthalpy depending on the choices of different parameters. Existence of negative enthalpy indicates that the system in this case is not a physical one. Therefore, in this case (presence of two roots for enthalpy), small and large black holes will be physical whereas the medium black holes will be non-physical. Since we could not obtain the root of mass analytically, we employ numerical calculations and present the results in various diagrams (see Fig. 3).

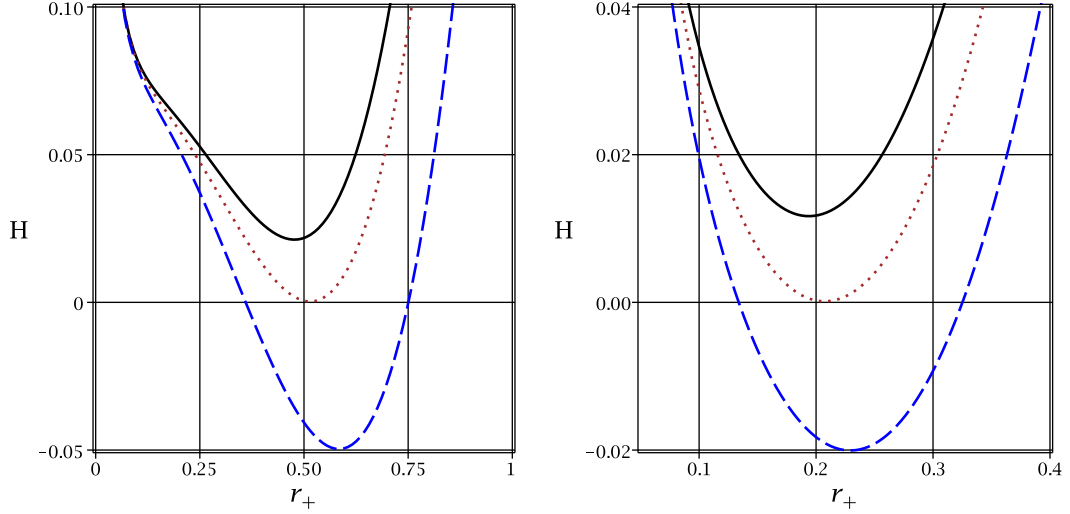


FIG. 3: H versus r_+ for $P = 0.5$, $\Phi_E = 1$, $q_M = 0.1$, $m = 1$, $c = 1$ and $k = 1$;
Left diagram: for $c_2 = 1$, $c_1 = -8$ (continuous line), $c_1 = -8.34$ (dotted line) and $c_1 = -9$ (dashed line).
Right diagram: for $c_1 = 1$, $c_2 = -0.4$ (continuous line), $c_2 = -0.515$ (dotted line) and $c_2 = -0.7$ (dashed line).

B. Temperature

Another thermodynamic quantity of interest is temperature. Taking a closer look at the temperature, one can see that for large and small horizon radii, q_M and P are dominant terms, respectively. Since q_M term is negative and P term is positive, one can conclude that at least one root exists for the temperature. This root separates the non-physical solutions with negative temperature from physical black holes with positive temperature. Therefore, there exists a condition for having physical black holes with positive temperature which is

$$8\pi P r_+^4 + m^2 c_1 c r_+^3 + (k^2 - \Phi_E^2 + m^2 c_2 c^2) r_+^2 - q_M^2 > 0. \quad (31)$$

It is worthwhile to mention that the presence of q_M leads the temperature to diverge toward $-\infty$ in the limit of $r_+ \rightarrow 0$, faster. This is one of the effects of the presence of magnetic charge. In addition, one can see that c_1 in temperature is not coupled with horizon radius. Here, it merely plays the role of a constant. Due to the coupling of different parameters with varying orders of horizon radius, for every specific ranges of horizon radius, one of these terms could be dominant. This may lead to the presence of extrema for the temperature. It is straightforward to show that the extrema of temperature are given by

$$r_{Extremum-T} = \sqrt{\frac{m^2 c^2 c_2 - \Phi_E^2 + k \pm \sqrt{m^2 c^2 c_2 (2k + m^2 c^2 c_2 - 2\Phi_E^2) + \Phi_E^4 + k(k - 2\Phi_E^2) - 96 P \pi q_M^2}}{16 P \pi}}. \quad (32)$$

The above obtained extrema for the temperature indicate that by suitable choices of different parameters, it may be possible to have one of the following cases:

- I) Temperature being only an increasing function of the horizon radius without any extremum.
- II) Existence of only one extremum with one root for the temperature.
- III) Presence of one minimum and one maximum with one root for the temperature.

We will investigate these cases later in a separate section with some diagrams for more clarifications.

$q_M \rightarrow 0$ limit:

In the absence of magnetic charge, it is possible to derive an interesting property for these black holes. In the expression for temperature, k , Φ_E and c_2 are coupled with horizon radius of the same order. In the absence of the magnetic charge, the dominant terms for small values of horizon radius will be

$$m^2 c_2 c^2 + k - \Phi_E^2. \quad (33)$$

Now, it is possible to tune this relation in a way so that it vanishes. If we eliminate this relation, one can find the

following relation for temperature

$$T = 2r_+P + \frac{m^2cc_1}{4\pi}, \quad (34)$$

which for the limit of $r_+ \rightarrow 0$, it is non-zero.

Remembering that in the evaporation of black holes by the Hawking radiation mechanism, the horizon radius eventually vanishes. However, we see here that in this case, there will be a remnant for the temperature of black holes. This indicates that all the information regarding existence of the black holes is not vanished completely despite the statement of paradox information. In fact, a trace of existence of black holes will remain which presents itself as a fluctuation in temperature of the background spacetime where black hole was present. This specific property for the temperature is due to the existence of massive gravitons. This shows that generalization from massless gravitons to massive ones, introduces new properties to the thermodynamics of black holes which could solve and answer some long standing questions regarding the physics of black holes such as the information paradox. It is worthwhile to mention that existence of the remnant for temperature of the black holes, to our knowledge, so far was only reported for black holes in the context of massive gravity [63] and it is one of the unique properties of the massive gravity which make it different from other modified theories of the gravity.

C. Heat Capacity

Our next thermodynamical quantity of interest is the heat capacity. This quantity is of interest because of two important properties; sign and divergencies. Basically, the conditions regarding the stability of black holes could be attained by studying the sign of the heat capacity. Regardless of other parameters of the black holes, the negativity of it shows that black holes are thermally unstable while the vice versa is true for stability. On the other hand, it has been argued that black holes go under second order phase transitions where they meet divergencies of the heat capacity. Since we are working in extended phase space, the heat capacity is given by

$$C_{Q,P} = \frac{T}{\left(\frac{\partial^2 M}{\partial S^2}\right)_{Q,P}} = T \left(\frac{\partial S}{\partial T}\right)_{Q,P} = T \frac{\left(\frac{\partial S}{\partial r_+}\right)_{Q,P}}{\left(\frac{\partial T}{\partial r_+}\right)_{Q,P}}. \quad (35)$$

By using the temperature (17) and entropy (28), one can obtain the heat capacity of massive charged dyonic black holes as

$$C_{Q,P} = 2\pi r_+^2 \frac{m^2 c r_+^2 (c_2 c + c_1 r_+) - \Phi_E^2 r_+^2 - q_M^2 + k r_+^2 + 8\pi r_+^4 P}{\Phi_E^2 r_+^2 + 3q_M^2 + 8\pi r_+^4 P - m^2 r_+^2 c_2 c^2 - k r_+^2}. \quad (36)$$

In order to have a positive heat capacity, the numerator and denominator of heat capacity must be whether both negative or positive. The numerator of heat capacity is exactly the same with positive condition that we found for the temperature (see Eq. (31)). Since this relation is supposed to be positive, the denominator must also be positive to have a positive heat capacity, and hence, thermally stable solutions. Therefore, we have

$$\Phi_E^2 r_+^2 + 3q_M^2 + 8\pi r_+^4 P - m^2 r_+^2 c_2 c^2 - k r_+^2 > 0,$$

in which by combining it with previous condition for having positive numerator, we obtain

$$0 < m^2 c_2 c^2 r_+^2 + r_+^3 m^2 c_1 c - \Phi_E^2 r_+^2 - q_M^2 + k^2 r_+^2 + 8\pi P r_+^4 < r_+^3 m^2 c_1 c - 2q_M^2. \quad (37)$$

In conclusion, if Eq. (37) is satisfied, the heat capacity will be positive and black holes are thermally stable. On the other hand, divergencies of the heat capacity are obtained according to the following relation

$$r_{\infty-C_{Q,P}} = \sqrt{\frac{m^2 c^2 c_2 - \Phi_E^2 + k \pm \sqrt{m^2 c^2 c_2 (2k + m^2 c^2 c_2 - 2\Phi_E^2) + \Phi_E^4 + k(k - 2\Phi_E^2) - 96\pi P q_M^2}}{16P\pi}}. \quad (38)$$

Evidently, depending on the choices of different parameters, the heat capacity may come across one of the following cases:

- I) Absence of divergency which is observed when it is not real valued.

II) Presence of only one divergency which takes place only when the following conditions for different parameters hold simultaneously

$$m^2 c^2 c_2 (2k + m^2 c^2 c_2 - 2\Phi_E^2) + \Phi_E^4 + k (k - 2\Phi_E^2) - 96 P \pi q_M^2 = 0,$$

$$m^2 c^2 c_2 - \Phi_E^2 + k > 0.$$

III) Existence of two divergencies. This case happens if both positive and negative branches of the obtained solutions are positive and real valued. Therefore, another set of conditions are imposed for negative branch as well which are

$$m^2 c^2 c_2 (2k + m^2 c^2 c_2 - 2\Phi_E^2) + \Phi_E^4 + k (k - 2\Phi_E^2) - 96 \pi P q_M^2 > 0,$$

$$m^2 c^2 c_2 - \Phi_E^2 + k \pm \sqrt{m^2 c^2 c_2 (2k + m^2 c^2 c_2 - 2\Phi_E^2) + \Phi_E^4 + k (k - 2\Phi_E^2) - 96 \pi P q_M^2} > 0.$$

Returning to the obtained divergency, let's examine different limiting cases. First of all, interestingly, the magnetic charge, q_M is coupled with pressure and the only trace of the pressure in numerator is due to this term. In the absence of the magnetic charge, divergencies will be only decreasing functions of the pressure. This highlights the contribution and the effect of the magnetic charge in thermodynamical phase transition of these black holes. It is worthwhile to mention that magnetic charge term is negative and its contribution is toward decreasing the value of divergencies. On the other hand, for the electric part of solutions, except for Φ_E^4 , all the other terms including electric part contribute to negativity of the obtained divergencies. In the absence of electric part, for positive branches of the solutions, only magnetic charge term contributes to negativity. Finally, the massive terms only contribute to positivity of the divergencies. This shows that thermodynamical phase transitions more likely take place in larger horizon radius for massive graviton cases compared to massless ones. This is one of the contributions of the massive gravity in thermodynamical structure of the black holes. Later, we will present some diagrams and give interpretations regarding the thermodynamical behavior of black holes for mentioned divergencies, and hence, phase transitions. It is worthwhile to mention that obtained divergencies for the heat capacity are the same as extrema that were extracted for temperature (32).

D. Free energy

The free energy is considered to be one of the thermodynamical potentials which could be used to derive other thermodynamical quantities. The free energy could also be employed to extract information regarding the phase transitions of the black holes and their chemical equilibrium. Thermodynamically speaking, when a system reaches chemical equilibrium at constant temperature and pressure, its free energy minimizes. This means that the presence of an extremum in free energy diagrams indicates that system undergoes a second order phase transition in that extremum. This point is known as equilibrium point and derivative of the free energy with respect to thermodynamical coordinate vanishes there.

Using the obtained free energy (30), it is a matter of calculation to show that roots of free energy are

$$r_{root-W} = \sqrt[3]{\frac{k + c^2 m^2 c_2 - \Phi_E^2 \pm \sqrt{32 P \pi q_M^2 + m^2 c^2 c_2 (2k + m^2 c^2 c_2 - 2\Phi_E^2) + \Phi_E^4 + k (k - 2\Phi_E^2)}}{16 \pi P}}. \quad (39)$$

Obtained roots for the free energy are almost identical with obtained divergencies for the heat capacity with a few differences. Here, magnetic charge term coupled with pressure is positive and therefore, its contribution is toward increasing the values of root. Otherwise, same arguments that were mentioned for divergencies of the heat capacity, regarding the effects of different parameters, are valid for the roots of free energy as well.

The equilibrium points for these black holes could be obtained by using the first derivative of the free energy with respect to thermodynamical coordinates. Here, we choose horizon radius as our thermodynamical coordinate which leads to following equilibrium points

$$r_{Equilibrium-W} = \sqrt{\frac{m^2 c^2 c_2 - \Phi_E^2 + k \pm \sqrt{m^2 c^2 c_2 (2k + m^2 c^2 c_2 - 2\Phi_E^2) + \Phi_E^4 + k (k - 2\Phi_E^2) - 96 P \pi q_M^2}}{16 P \pi}}. \quad (40)$$

A simple comparison shows that obtained equilibrium points are identical to extrema and divergencies which were extracted for the temperature and the heat capacity, respectively. Now, since we have two roots and two extrema for the free energy, one of these cases may happen:

- I) Existence of two roots and one extremum.
- II) Presence of two roots and two extrema.
- III) Absence of extremum and existence of only one root.
- IV) Absence of extremum and root.

We will plot some diagrams to elaborate mentioned cases later. So, we temporarily postpone the discussions here.

IV. VAN DER WAALS LIKE BEHAVIOR

Replacing the cosmological constant with its corresponding pressure provides the possibility of studying the critical behavior of black holes in the context of van der Waals like characteristic. Here, by replacing the cosmological constant in the temperature, we will obtain the equation of the state in the following form

$$P = \frac{1}{8\pi} \left[\frac{\Phi_E^2}{r_+^2} + \frac{q_M^2}{r_+^4} - \frac{k}{r_+^2} + \frac{4T}{r_+} - m^2 c \left(\frac{cc_2}{r_+^2} - \frac{c_1}{r_+} \right) \right]. \quad (41)$$

As it was pointed out earlier, the total volume of the black hole, conjugate to pressure, is obtainable in terms of the horizon radius. Therefore, it is possible to obtain the equation of state as

$$P = \frac{\Phi_E^2}{12} \sqrt[3]{\frac{6}{\pi V^2}} + \frac{T}{6} \sqrt[3]{\frac{36\pi}{V}} - \frac{k}{12} \sqrt[3]{\frac{6}{\pi V^2}} - \frac{m^2 c \left(2\sqrt[3]{\pi} cc_2 + \sqrt[3]{6V} c_1 \right)}{24} \sqrt[3]{\frac{6}{\pi^2 V^2}} + \frac{q_M^2}{18} \sqrt[3]{\frac{36\pi}{V^4}}. \quad (42)$$

Before we study the possible existence of the van der Waals like critical behavior, let us examine the effects of different parameters on the pressure.

Evidently, the massive terms have negative effect on the value of the pressure. This indicates that generalization from massless to massive gravitons leads to decrease the thermodynamical pressure of black holes. Contrary to massive terms, electric and magnetic parts of the solutions have positive contributions into values of the pressure. Especially for small values of horizon radius, the contribution of magnetic charge term becomes highly significant.

As for topological term (k -term), its contribution depends on the choices of topology. For spherical case, it will decrease the value of the pressure while the opposite is observed for hyperbolic horizon. Regarding T -term, we should note that since positive values of the temperature are valid for the black holes, its contribution is always positive.

It is worthwhile to mention that due to specific coupling of different factors of horizon radius with different terms, by suitable choices, it is possible to cancel the effects of some of terms. In other words, if the following equations hold simultaneously,

$$4\pi T - m^2 cc_1 = 0,$$

$$\Phi_E^2 - m^2 c^2 c_1 - k = 0,$$

the pressure will be only a function of the magnetic charge.

In order to study the critical behavior of the system, we use specific volume which is related to horizon radius, $r_+ = v/2$. Therefore, hereafter we work with the following equation of state

$$P = \frac{1}{2\pi} \left[\frac{\Phi_E^2}{v^2} + \frac{4q_M^2}{v^4} - \frac{k}{v^2} + \frac{2T}{v} - m^2 c \left(\frac{cc_2}{v^2} - \frac{c_1}{2v} \right) \right]. \quad (43)$$

We are in now a position to study possible phase transition and van der Waals like behavior for these black holes.

A. Van der Waals like phase transition

The first step for studying van der Waals like behavior of the black holes is obtaining their critical points. To do so, we employ the properties of $P - v$ diagrams which is known as inflection point with the following properties

$$\left(\frac{\partial P}{\partial v} \right)_T = \left(\frac{\partial^2 P}{\partial v^2} \right)_T = 0. \quad (44)$$

Using obtained equation of the state (43) with properties of inflection point (44), one can obtain the following relation for calculating critical volume

$$(m^2 c^2 c_2 - \Phi_E^2 + k) v^2 - 24q_M^2 = 0. \quad (45)$$

It is a matter of calculation to obtain critical volume as

$$v_c = \frac{12q_M}{\sqrt{6m^2 c^2 c_2 - 6\Phi_E^2 + 6k}}. \quad (46)$$

By employing calculated critical volume, one can find the critical values of temperature, pressure and free energy which take the following forms

$$T_c = \frac{m^2 c c_1}{4\pi} + \frac{\sqrt{6}(m^2 c^2 c_2 - \Phi_E^2 + k)^{\frac{3}{2}}}{12\pi q_M} - \frac{\sqrt{6}(m^2 c^2 c_2 - \Phi_E^2 + k)^{\frac{3}{2}}}{216\pi q_M}, \quad (47)$$

$$P_c = \frac{(m^2 c^2 c_2 - \Phi_E^2 + k)^2}{96\pi q_M^2} \quad (48)$$

$$W_c = \frac{2q_M}{\sqrt{6}} \sqrt{(m^2 c^2 c_2 - \Phi_E^2 + k)}. \quad (49)$$

In addition, the universal ratio of $\frac{P_c v_c}{T_c}$ for these black holes will be obtained as

$$\frac{P_c v_c}{T_c} = \frac{\frac{3}{4}\sqrt{6}}{2\sqrt{6} + 9m^2 c c_1 q_M^2 (m^2 c^2 c_2 - \Phi_E^2 + k)^{-3/2}}, \quad (50)$$

which is modified in the presence of massive term. In the absence of massive terms, Eq. (50) reduces to the universal ration of Reissner Nordström black holes [89].

Before we proceed, it is necessary to study the obtained critical values. The critical volume is an increasing function of the magnetic charge and electric part of the solutions while it is a decreasing function of the massive parameter. The effect of the topological term is depending on the choice of topology. For spherical horizon, critical horizon radius is a decreasing function of the topological term while the opposite is observed for hyperbolic horizon. As one can see, generalization to massive gravity has interesting effects on critical behavior of the system. The most important contribution is that critical behavior could be observed for non-spherical horizons as well. Previously, it was shown that van der Waals like behavior is only observable for spherical black holes whereas black holes with other type of horizons suffer the absence of such behavior in their phase diagrams. Here, the generalization from massless gravitons to massive ones, provides the possibility of van der Waals like behavior for black holes with different horizon. In other words, the topological restriction for having van der Waals like behavior for black holes is relaxed. Here, the existence of real valued critical volume is restricted by the following condition

$$m^2 c^2 c_2 - \Phi_E^2 + k > 0.$$

In other words, it is possible to eliminate critical behavior for these black holes with suitable choices of different parameters. Another interesting fact is that critical volume does not depend on the variations of c_1 . In other words, generalization to massive gravity has no effect on the critical volume. Finally, it is worth mentioning again that critical horizon radius is a decreasing function of the massive gravity. These are the effects of massive parameter on the critical volume.

As for the critical temperature, contrary to the critical volume, it is a decreasing function of the magnetic charge and electric part while it is an increasing function of the massive parameter. The effects of different topologies are also opposite to what were observed for critical volume. Interestingly, the critical temperature is c_1 dependent and it is an increasing function of this parameter. The existence of positive critical temperature is restricted by the following condition

$$m^2 c c_1 v_c^3 + (4m^2 c^2 c_2 - 4\Phi_E^2 + 4k) v_c^2 - 32q_M^2 > 0,$$

which shows that it is possible to have positive critical volume with negative critical temperature (by suitable choice of magnetic charge).

Due to specific structure of the critical pressure, it is always positive. The critical pressure is also independent of variation of the c_1 parameter which could be employed to make previous comments for this critical value as well. In addition, here too, critical pressure is a decreasing function of the magnetic charge and Φ_E , while it is an increasing function of the massive parameter and topological factor.

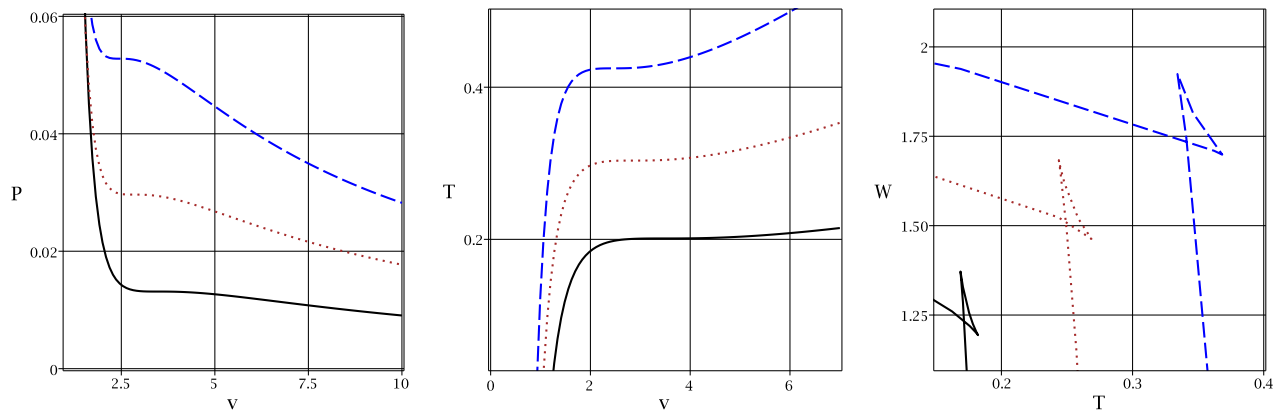


FIG. 4: $P - v$ (left), $T - v$ (middle) and $W - T$ (right) diagrams for $m = 0.5$, $c = c_1 = 2$, $c_2 = 3$, $\Phi_E = 0.1$ and $q_M = 0.1$; $k = -1$ (continuous line), $k = 0$ (dotted line) and $k = 1$ (dashed line). $P - v$ diagram for $T = T_c$, $T - v$ diagram for $P = P_c$ and $W - T$ diagram for $P = 0.5P_c$.

Finally, obtained critical free energy shows that its value is always positive (if previous condition for having real valued critical horizon radius is satisfied). In addition, it is an increasing function of the massive parameter, magnetic charge and topological factor while it is a decreasing function of the electric charge.

To elaborate the existence of van der Waals like behavior for different topological black holes, we plot phase diagrams for obtained critical values (see Fig. 4).

Formation of swallow-tail shape for $W - T$ (right panel of Fig. 4), existence of inflection point for $P - v$ (left panel of Fig. 4) and presence of subcritical isobars in $T - v$ diagrams (middle panel of Fig. 4), indicate that these black holes with different topological structures, enjoy second order phase transition and van der Waals like behavior in their phase diagrams. This is a new achievement which is seen in massive gravity context [146].

B. Limiting cases and van der Waals like behavior for non-spherical black holes

In previous studies regarding the dyonic black holes, it was pointed out that planar black holes suffer the absence of van der Waals like phase transition in their phase diagrams. Here, in previous section, it was shown that generalization to massive gravity solves this problem and introduces van der Waals like phase transition into phase structure of the black holes with hyperbolic and flat horizons. This possibility opens up new avenues in studying different aspects of black holes with application in gauge/gravity duality. In the AdS/CFT correspondence, l is interpreted as a measure of the number of degrees of freedom, N , of the boundary field theory and its relation is determined by the CFTs under consideration. That being said, some authors consider that varying in pressure, hence Λ , corresponds to vary the number of colors, N , in the boundary Yang-Mills theory and the volume conjugating to pressure in the boundary field theory is equivalent to an associated chemical potential for color [98, 147, 148]. Another approach considers the variation in Λ corresponds to variation of the volume on which the field theory resides [149]. Some of the applications of extended phase space and Van der Waals like behavior in AdS/CFT are in the context of; Holographic superconductors [150], Holographic entanglement entropy [151] and etc. Later, we will show that different approaches in studying critical behavior of the black holes yield consistent results. Here, the effects of the variation of the magnetic charge, q_M , on van der Waals like behavior of these black holes in fixed Φ_E ensemble are studied.

We have plotted three sets of figures for hyperbolic (Fig. 5), flat (Fig. 6) and spherical (Fig. 7) cases. These figures contain $P - v$ (left panels), $T - v$ (middle panels) and $W - T$ (right panels) diagrams. In these diagrams, electric part, pressure and massive parameter are considered to be fixed and variation of the magnetic charge is studied.

First, we take $W - T$ diagrams into account. Evidently, for large values of electromagnetic charge, no phase transition exists and only one phase is observable for black holes (left panels of Figs. 5-7, dashed-dotted lines). The formation of two phases and van der Waals like behavior could be observed by decreasing magnetic charge till it meets a critical magnetic charge, q_{M_c} (left panels of Figs. 5-7, dashed lines). Here, a phase transition of small/large black holes takes place. For magnetic charges smaller than critical magnetic charge, an unstable phase is formed. Therefore, in this case, three phases exist which are small, medium and large black holes. This could be observed in $W - T$ diagrams as formation of the swallow-tail (left panels of Figs. 5-7, dotted lines). Finally, for the limit $q_M \rightarrow 0$, all the three phases reduces to two phases for black holes (left panels of Figs. 5-7, continuous lines) in which the smaller black holes are unstable while the larger ones are stable.

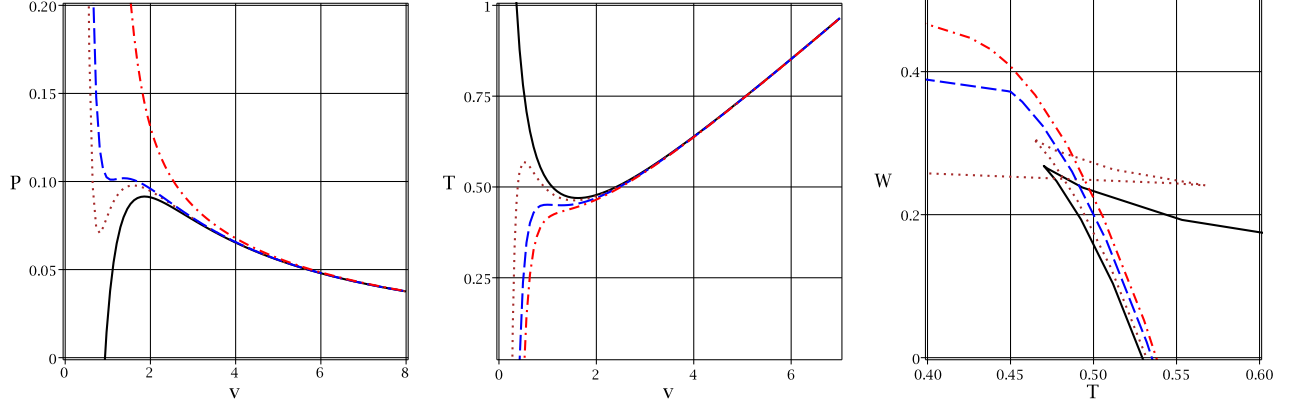


FIG. 5: $P - v$ (left), $T - v$ (middle) and $W - T$ (right) diagrams for $m = 0.5$, $c = c_1 = 2$, $c_2 = 3$, $\Phi_E = 0.1$ and $k = -1$; For $T - v$ and $W - T$ panels: $P=0.12$, $q_M = 0$ (continuous line), $q_M = 0.2$ (dotted line), $q_M = 0.32$ (dashed line) and $q_M = 0.4$ (dashed-dotted line). For $P - v$ panel: $T=0.42$, $q_M = 0$ (continuous line), $q_M = 0.3$ (dotted line), $q_M = 0.35$ (dashed line) and $q_M = 1$ (dashed-dotted line).

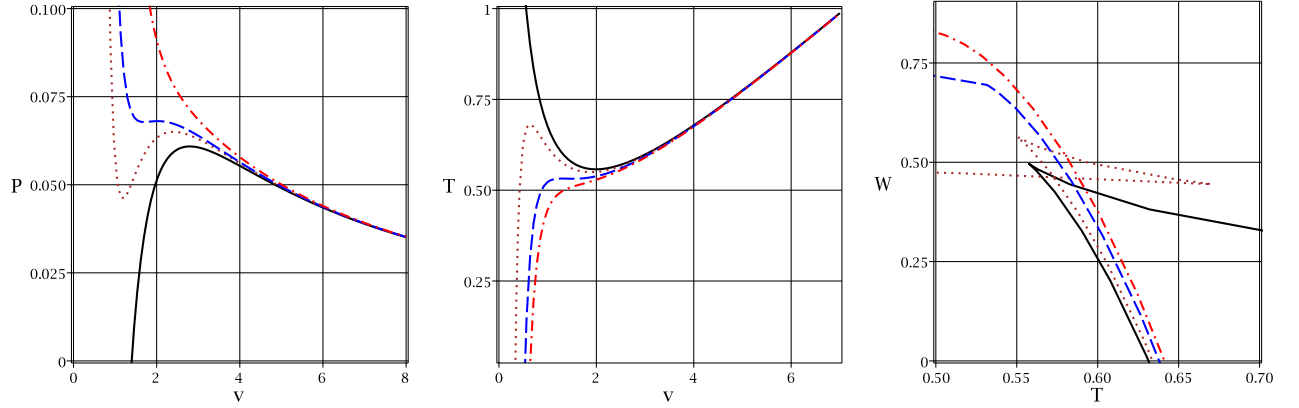


FIG. 6: $P - v$ (left), $T - v$ (middle) and $W - T$ (right) diagrams for $m = 0.5$, $c = c_1 = 2$, $c_2 = 3$, $\Phi_E = 0.1$ and $k = 0$; For $T - v$ and $W - T$ panels: $P=0.12$, $q_M = 0$ (continuous line), $q_M = 0.3$ (dotted line), $q_M = 0.49$ (dashed line) and $q_M = 0.6$ (dashed-dotted line). For $P - v$ panel: $T=0.42$, $q_M = 0$ (continuous line), $q_M = 0.55$ (dotted line), $q_M = 0.65$ (dashed line) and $q_M = 1$ (dashed-dotted line).

Now, we study $T - v$ diagrams. Evidently, here too, for the magnetic charges larger than the critical magnetic charge, the temperature is only an increasing function of the volume without any subcritical isobar and extremum. Here, only one stable phase is possible for black holes (middle panels of Figs. 5-7, dashed-dotted lines). For critical magnetic charge, an extremum is observed and a subcritical isobar is formed (middle panels of Figs. 5-7, dashed lines). The extremum separates small and large phases from each other. For $0 < q_M < q_{M_c}$, two extrema are formed for $T - v$ diagrams. The unstable phase of medium black holes is located between these two extrema and small and large phases are located before maximum and after minimum, respectively (middle panels of Figs. 5-7, dotted lines). Interestingly, for $q_M \rightarrow 0$, the behavior of the temperature is modified. Here, a minimum is observable for the temperature in which the phase before this minimum is the unstable one (middle panels of Figs. 5-7, continuous lines). At the minimum a phase transition to larger stable black holes takes place.

For $P - v$ diagrams, in case of $q_M > q_{M_c}$, the pressure is only a decreasing function of the volume without any extremum which indicates that only a single stable phase exists (left panels of Figs. 5-7, dashed-dotted lines). For $q_M = q_{M_c}$, inflection point is formed and two phases of small and large stable black holes are separated (left panels of Figs. 5-7, dashed lines). The case $0 < q_M < q_{M_c}$ leads to appearance of two extrema where the unstable medium black hole phase is located between them (left panels of Figs. 5-7, dotted lines). Finally, in the absence of magnetic charge, the thermodynamical behavior of the pressure is modified and a maximum is formed. The maximum marks

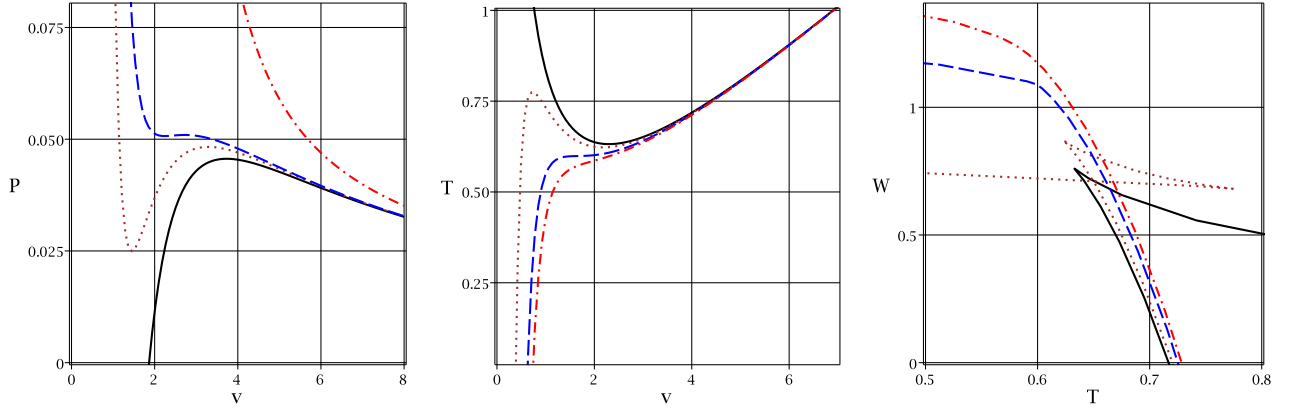


FIG. 7: $P - v$ (left), $T - v$ (middle) and $W - T$ (right) diagrams for $m = 0.5$, $c = c_1 = 2$, $c_2 = 3$, $\Phi_E = 0.1$ and $k = 1$; For $T - v$ and $W - T$ panels: $P=0.12$, $q_M = 0$ (continuous line), $q_M = 0.4$ (dotted line), $q_M = 0.67$ (dashed line) and $q_M = 0.8$ (dashed-dotted line). For $P - v$ panel: $T=0.42$, $q_M = 0$ (continuous line), $q_M = 0.8$ (dotted line), $q_M = 1$ (dashed line) and $q_M = 4$ (dashed-dotted line).

the phase transition between unstable small black holes and stable large black holes.

Here, we see that modifications in thermodynamical structure of the black holes for non-spherical black holes are similar to those that are observed for spherical ones. This similarity shows that non-spherical black holes also enjoy van der Waals like behavior in their phase diagrams. It is worthwhile to mention that critical values and the places of mentioned modification depends on choices of the topology. Later, we will present more details regarding different phases in various comparative diagrams.

C. Alternative method for studying van der Waals like behavior

Instead of using the equation of state and properties of inflection point for studying critical behavior of the black holes, it is possible to use another method which uses the slope of temperature versus entropy. This method was first introduced in Ref. [152] and employed in several other papers. It was shown that the results of this method are consistent with other methods. Here we examine the validity of this method in dyonic massive gravity.

The method employs the slope of temperature versus entropy to derive a new relation for the pressure which is independent of the equation of state. If the new relation admits a maximum, the black holes enjoy second order phase transition and van der Waals like behavior in their phase space. The phase transition point is located at the maximum and its pressure corresponds to the critical pressure.

For these black holes, the new relation for pressure by using the heat capacity (36) is

$$P_{New} = \frac{(m^2 c^2 c_2 - 4 \Phi_E^2 + 4k) v_c^2 - 12 q_M^2}{2\pi v^4}. \quad (51)$$

We should note that the subscript "NEW", simply, stands for the new method that we have used to obtain pressure and temperature. The maximum pressure and its corresponding volume are obtained, respectively, in following forms

$$v_{Maximum} = \frac{12q_M}{\sqrt{6m^2 c^2 c_2 - 6\Phi_E^2 + 6k}}, \quad (52)$$

$$P_{Maximum} = \frac{(m^2 c^2 c_2 - \Phi_E^2 + k)^2}{96\pi q_M^2}, \quad (53)$$

which are exactly critical horizon volume and pressure that were extracted in previous section (see Eqs. (46) and (48)). This shows that the results of this method are consistent with those derived in previous section and this method provides satisfactory results. Now, replacing pressure in the temperature (17) with Eq. (51), one can find a relation independent of pressure for the temperature

$$T_{New} = \frac{m^2 c c_1 v^3 + 4(m^2 c^2 c_2 - \Phi_E^2 + k) v^2 - 32 q_M^2}{4\pi v^3}. \quad (54)$$

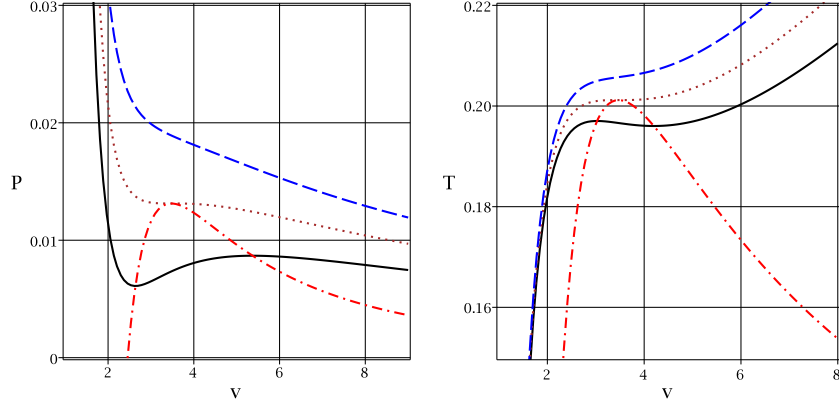


FIG. 8: For $m = 0.5$, $c = c_1 = 2$, $c_2 = 3$, $\Phi_E = 0.1$, $q_M = 0.1$ and $k = -1$;

Left panel: P_{new} (dashed-dotted line) and P diagrams versus v for $T = 0.9T_c$ (continuous line), $T = T_c$ (dotted line) and $T = 1.1T_c$ (dashed line).

Right panel: T_{new} (dashed-dotted line) and T diagrams versus v for $P = 0.9P_c$ (continuous line), $P = P_c$ (dotted line) and $P = 1.1P_c$ (dashed line).

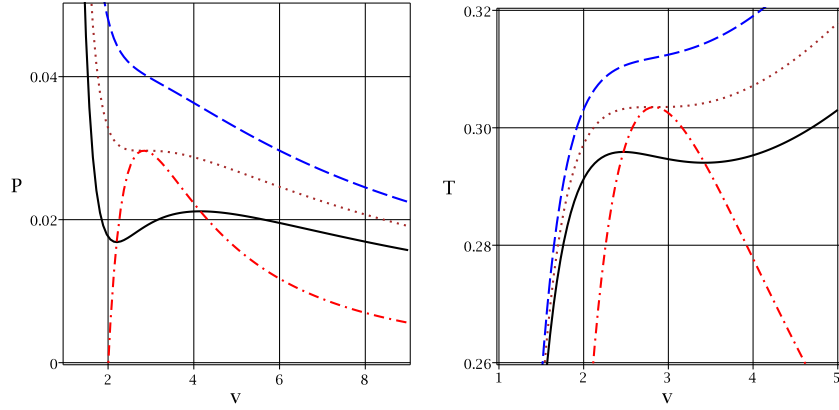


FIG. 9: For $m = 0.5$, $c = c_1 = 2$, $c_2 = 3$, $\Phi_E = 0.1$, $q_M = 0.1$ and $k = 0$;

Left panel: P_{new} (dashed-dotted line) and P diagrams versus v for $T = 0.9T_c$ (continuous line), $T = T_c$ (dotted line) and $T = 1.1T_c$ (dashed line).

Right panel: T_{new} (dashed-dotted line) and T diagrams versus v for $P = 0.9P_c$ (continuous line), $P = P_c$ (dotted line) and $P = 1.1P_c$ (dashed line).

Using manual calculations, it can be shown that the new relations for the temperature and pressure coincide with usual T and P , which is in agreement with the existence of a single temperature (and also pressure in an extended phase space) in the dual CFT. Replacing volume with obtained maximum volume, one can find the following (maximum) temperature which is essentially the critical temperature

$$T_{Maximum} = \frac{27m^2cc_1q_M + (6m^2c^2c_2 - 6\Phi_E^2 + 6k)^{\frac{3}{2}}}{108\pi q_M}. \quad (55)$$

Numerical evaluation shows that this temperature and critical temperature which was obtained in previous section are the same and therefore, we are able to extract critical temperature using this method.

It is evident that by using the method which was employed in this section, one can extract relations for temperature and pressure which are independent of each other and it is different from equation of the state. In addition, these new relations could be employed to plot new $T - v$, $P - v$ and $P - T$ diagrams which are different from previous phase diagrams. This enables one to study other thermodynamical properties of the black holes which were not possible to investigate due to limitations of the previous methods. In order to elaborate this matter, we will plot some diagrams (Figs. 8-11).

First of all, as one can see, the maxima of the new relations for the temperature and pressure are the critical

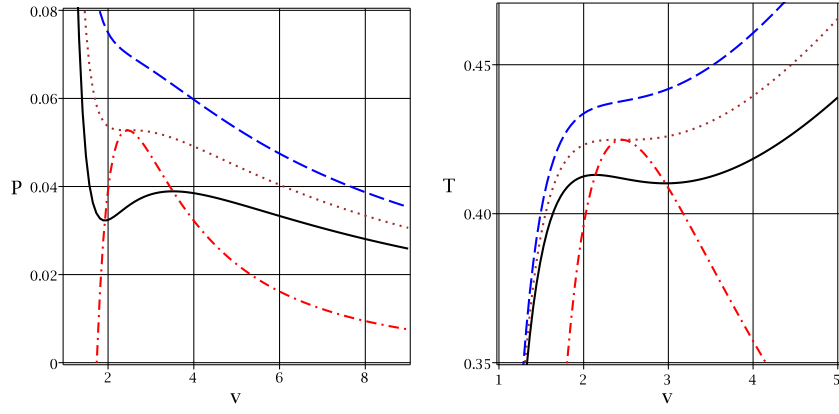


FIG. 10: For $m = 0.5$, $c = c_1 = 2$, $c_2 = 3$, $\Phi_E = 0.1$, $q_M = 0.1$ and $k = 1$;

Left panel: P_{new} (dashed-dotted line) and P diagrams versus v for $T = 0.9T_c$ (continuous line), $T = T_c$ (dotted line) and $T = 1.1T_c$ (dashed line).

Right panel: T_{new} (dashed-dotted line) and T diagrams versus v for $P = 0.9P_c$ (continuous line), $P = P_c$ (dotted line) and $P = 1.1P_c$ (dashed line).

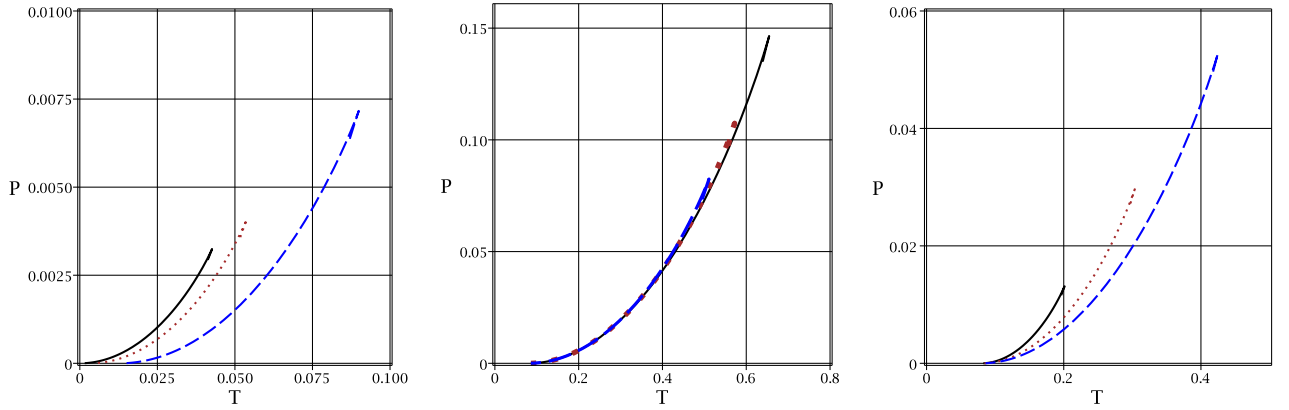


FIG. 11: P versus T diagrams for $c = c_1 = 2$, $c_2 = 3$ and $\Phi_E = 0.1$;

Left panel: $k = 1$, $q_M = 1$, $m = 0$ (continuous line), $m = 0.1$ (dotted line) and $m = 0.2$ (dashed line).

Middle panel: $k = 1$, $m = 0.5$, $q_M = 0.6$ (continuous line), $q_M = 0.7$ (dotted line) and $q_M = 0.8$ (dashed line).

Right panel: $q_M = 1$, $m = 0.5$, $k = -1$ (continuous line), $k = 0$ (dotted line) and $k = 1$ (dashed line).

temperature and pressure, respectively. For the pressures and temperatures smaller than the critical pressure and temperature, the plotted diagrams for new relations include all the possible phase transition points that these black holes can acquire and the results of the new relations are consistent with those derived in previous section. In addition, we see that for the pressures and temperatures larger than the critical pressure and temperature, no phase transition exists.

On the other hand, $P - T$ diagrams are also plotted for more clarifications. These diagrams contain information regarding the region of equilibrium between two different phases which phase transitions takes place between them. These two phases are small and large black holes. The critical pressure and temperature are located at the end of these diagrams and beyond these two critical values, no phase transition takes place. Evidently, the equilibrium region is an increasing function of the massive parameter (left panel of Fig. 11) and topological factor (right panel of Fig. 11) while it is a decreasing function of magnetic charge (middle panel of Fig. 11).

D. Volume expansion coefficient, isothermal compressibility coefficient and speed of sound

Our final study in this section is obtaining specific properties of the critical systems known as the length/area/volume expansion coefficients, $(\alpha_L/\alpha_A/\alpha_V)$, the isothermal compressibility coefficient (κ_T) , and the speed of sound (c_s) .

The volume expansion coefficient for the black holes at constant pressure represents the change in the volume of black holes through the heat transferring. Here, the heat transferring could be detected by variation in the temperature of black holes. The length and area expansion coefficients for these black holes are given by

$$\alpha_L = \frac{1}{L} \left(\frac{\partial L}{\partial T} \right)_P \quad \& \quad \alpha_A = \frac{1}{A} \left(\frac{\partial A}{\partial T} \right)_P. \quad (56)$$

It is worthwhile mentioning that the length and area of a black hole recognize by the horizon radius (specific volume) and the total entropy, respectively. Therefore, one can rewrite α_L and α_A as

$$\alpha_L = \frac{1}{v} \left(\frac{\partial v}{\partial T} \right)_P \quad \& \quad \alpha_A = \frac{1}{S} \left(\frac{\partial S}{\partial T} \right)_P, \quad (57)$$

which for the obtained black hole solutions we can find

$$\alpha_A = 2\alpha_L, \quad (58)$$

and

$$\alpha_V = 3\alpha_L = \frac{1}{V} \left(\frac{\partial V}{\partial T} \right)_P = \frac{6v^3\pi}{2\pi P v^4 - v^2(m^2 c^2 c_2 - \Phi_E^2 + k) + 12q_M^2}, \quad (59)$$

which are consistent with the results of usual thermodynamic systems.

Besides, the isothermal compressibility coefficient represents variation in the volume of black holes corresponding to change in pressure. The isothermal term comes from the fact that we are dealing with system in the fixed temperature. For massive dyonic black holes, the isothermal compressibility coefficient can be written as [153]

$$\kappa_T = -\frac{1}{V} \left(\frac{\partial V}{\partial P} \right)_T = \frac{6v^4\pi}{2\pi P v^4 - v^2(m^2 c^2 c_2 - \Phi_E^2 + k) + 12q_M^2}, \quad (60)$$

in which we have used the following relation

$$\left(\frac{\partial V}{\partial P} \right)_T \left(\frac{\partial P}{\partial T} \right)_V \left(\frac{\partial T}{\partial V} \right)_P = -1. \quad (61)$$

Our next property of interest is the speed of sound. Here, the speed of sound represents a breathing mode for variation of the volume versus pressure while the area of the black holes remains fixed. In order to calculate this property of the black hole, first, we find the homogenous density of black holes by [154, 155]

$$\rho = \frac{M}{V} = \frac{8\pi P v^4 + 3m^2 v^3 c c_1 + (12\Phi_E^2 + 12k + 12m^2 c^2 c_2)v^2 + 48q_M^2}{8\pi v^4}. \quad (62)$$

Then, by using the following relation [154, 155],

$$\frac{1}{c_s^2} = \frac{\partial \rho}{\partial P}, \quad (63)$$

one can find that the speed of sound for massive dyonic black holes is

$$c_s^{-2} = 1 + \rho \kappa_T, \quad (64)$$

which is in permitted region of $0 \leq c_s^2 \leq 1$.

In order to finalize the discussions in this section, we will give some details regarding the obtained volume expansion and isothermal compressibility coefficients. Since the denominator of both these quantities are the same, we will limit our discussions to the volume expansion coefficient. First of all, it is a matter of calculation to show that divergencies of this quantity are located at

$$v_{\infty-\alpha} = \sqrt{\frac{m^2 c^2 c_2 - \Phi_E^2 + k \pm \sqrt{m^2 c^2 c_2 (2k + m^2 c^2 c_2 - 2\Phi_E^2) + \Phi_E^4 + k(k - 2\Phi_E^2) - 96\pi P q_M^2}}{4\pi P}}. \quad (65)$$

A simple comparison between obtained divergencies for the volume expansion coefficient and phase transition points (divergencies) that were extracted for the heat capacity (38) with $r = v/2$, one can conclude that they are identical.

In other words, phase transition points of heat capacity match with divergencies of the volume expansion coefficient. This shows that divergencies of the volume expansion coefficient are actually phase transition points. Therefore, studying this quantity would also provide the possibility of obtaining phase transition points.

The leading orders in near horizon and asymptotic limits for the volume expansion coefficient are in following forms, respectively,

$$\alpha_V|_{\text{very small } v} = \frac{\pi v^3}{2q_M^2} - \frac{\pi (\Phi_E^2 - m^2 c^2 c_2 - k) v^5}{24 q_M^4}, \quad (66)$$

$$\alpha_V|_{\text{very large } v} = \frac{3}{Pv} - \frac{3}{2} \frac{\Phi_E^2 - m^2 c^2 c_2 - k}{P^2 \pi v^3} + 3 \frac{(\Phi_E^2 - m^2 c^2 c_2 - k)^2}{4P^2 \pi} - \frac{6q_M^2}{P}. \quad (67)$$

Evidently, the near horizon limit is dominated by the magnetic charge. In the absence of magnetic charge, the near limit horizon will be modified as

$$\alpha_V|_{\text{very small } v} = \frac{6\pi v}{\Phi_E^2 - m^2 c^2 c_2 - k} - \frac{12\pi^2 P v^3}{(\Phi_E^2 - m^2 c^2 c_2 - k)^2}. \quad (68)$$

This highlights another effect of the magnetic charge in thermodynamical structure of the massive dyonic black holes. On the other hand, the leading order in asymptotic behavior of these black holes consists of pressure which is a decreasing function of it. Here, we see that in the presence of magnetic charge, the effects of the massive gravity present themselves in second leading terms. The exception is in the absence of the magnetic charge, in which the leading order of the near horizon limit consists of massive terms.

V. CONNECTION BETWEEN DIFFERENT PHASE DIAGRAMS

In this section, we would like to see how different thermodynamical quantities that were studied are related to each other and how we should interpret phase transitions and thermal stability conditions.

In studying temperature, heat capacity and free energy, it was shown that extrema of the temperature, divergencies of the heat capacity and equilibrium points of the free energy were located exactly at the same points. Remembering that divergencies of the heat capacity are points at which black holes suffer second order phase transitions, one can conclude that extrema in temperature and equilibrium points are also places in which black holes go under second order phase transitions. Therefore, studying these three quantities provides a uniform picture regarding thermodynamical behavior of the black holes. On the other hand, it was shown that different methods in studying van der Waals like behavior of these black holes lead to consistent results. In other words, the critical points that were extracted through different methods were identical.

Now, in order to show that positions (and number) of divergencies of the heat capacity are consistent with phase transition points (and number) in van der Waals like behavior, we have plotted various diagrams (see Figs. 12 and 13).

Interestingly, for the cases where van der Waals like diagrams ($P - r_+$) present an inflection point (pressure and temperature are the same as critical pressure and temperature), similarly, the heat capacity enjoys only one divergency in its diagrams (middle panels of Figs. 12 and 13). The places of this divergency and inflection point coincide which indicate that these two pictures are identical. Here, there is a coexistence state between two black holes (small/large black holes) with positive heat capacity.

On the other hand, when pressure and temperature are smaller than the critical pressure and temperature, a phase transition point is observed in the van der Waals diagrams. This phase transition point matches with that of heat capacity (left panels of Figs. 12 and 13). In other words, the places of unstable states in the van der Waals like diagrams are characterizing with the divergencies of the heat capacity. Interestingly, in this case, a region of instability (negative heat capacity) is formed between two divergence points. In previous case, only two stable phases existed which were small and large ones without any unstable region. Here, we have three regions which are small, medium and large black holes. In this case, medium black holes are unstable while small and large black holes are thermally stable. In previous case, there was a coexistence state between both phases, whereas here, a phase transition take place over a region which corresponds to medium black holes. If one considers the growth of the black holes, it could be pointed that upon growing to the size of smaller divergency, a phase transition takes place and size of the black holes changes to the size of the larger divergency whereas vice versa could be observed for Hawking radiation and evaporation of the black holes. Such sudden changes in the size of the black holes would leave its traces in gravitational

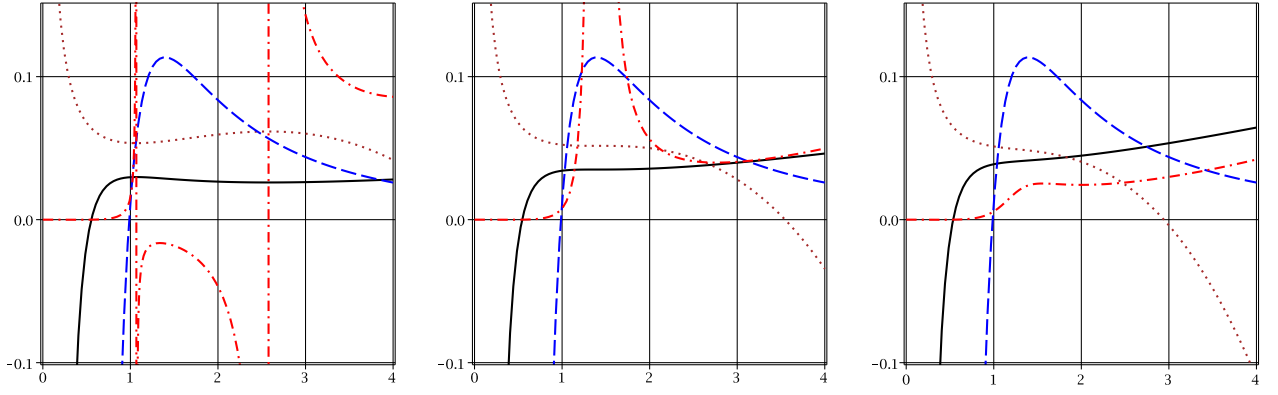


FIG. 12: T (continuous line), W (dotted line), P_{New} (dashed line) and C_P (dashed-dotted line) versus r_+ diagrams for $c = c_1 = 2$, $c_2 = 3$, $\Phi_E = 0.1$, $k = 1$, $m = 0.1$ and $q_M = 0.6$;
Left panel: $P = 0.5P_c$; **Middle panel:** $P = P_c$; **Right panel:** $P = 1.5P_c$.

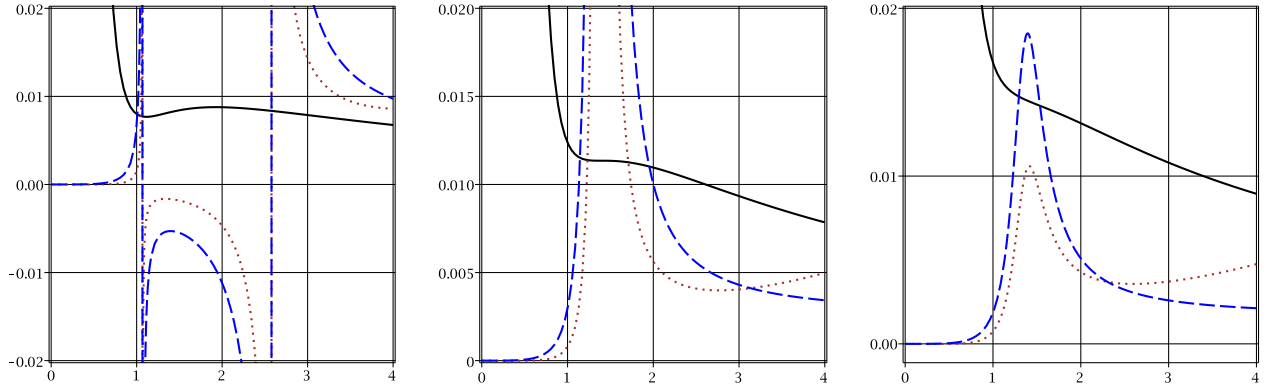


FIG. 13: P (continuous line), C_P (dotted line) and κ (dashed line) versus r_+ diagrams for $c = c_1 = 2$, $c_2 = 3$, $\Phi_E = 0.1$, $k = 1$, $m = 0.1$ and $q_M = 0.6$;
Left panel: $P - r_+$ diagram for $T = 0.9T_c$ and $C_P - r_+$ for $P = 0.5P_c$.
Middle panel: $P - r_+$ diagram for $T = T_c$ and $C_P - r_+$ for $P = P_c$.
Right panel: $P - r_+$ diagram for $T = 1.1T_c$ and $C_P - r_+$ for $P = 1.1P_c$.

properties of the black holes, such as gravitational wave and quasinormal modes. Recently, it was shown that quasinormal modes of the black holes acquire a dramatic change in the slopes of their frequencies in small and large black holes near the critical point where the Van der Waals like thermodynamic phase transition takes place [119, 156]. In fact, it was argued that the quasinormal mode can be a dynamic probe of the thermodynamic phase transition. Therefore, it might provide an observational potential to study thermodynamical structure of the black holes.

Finally, in the absence of phase transition in van der Waals like diagrams, heat capacity is smooth without any divergency (right panels of Figs. 12 and 13). Here, we see that the critical points that are extracted through different methods, are consistent and the obtained critical points in the heat capacity are places in which system has van der Waals like phase transition. This shows that the thermodynamical picture which is drawn by different methods for black holes are consistent with each other. It should be pointed out that, although the phase transition points for different methods are identical, every phase diagram describes a part of thermodynamical properties of the black holes. In order to have a complete picture regarding thermodynamical structure of the black holes, it is necessary to study different phase diagrams in more details.

Before, finishing this part, we will give more details regarding the possibility of existence of black holes for different phases. Previously, we observed that speed of sound must not exceed the speed of light. This could be acquired if isothermal compressibility coefficient is positive valued. In plotted diagrams for this quantity (Fig. 13), one can see that the divergencies of isothermal compressibility coefficient are identical to those obtained for the heat capacity. This shows that divergencies of the isothermal compressibility coefficient are marking a phase transition point which agrees

with our earlier results. For pressures smaller than critical pressure, isothermal compressibility coefficient has two divergencies. Between these two divergencies (medium black holes), isothermal compressibility coefficient is negative valued which leads to the fact that speed of sound will be more than unity, hence, more than the speed of light. This shows that the medium black holes, which are thermally unstable, have speed of sound larger than the speed of light. Therefore medium black holes do not have physical properties. In other words, although medium black holes have positive temperature and geometrically well behaved, they are not physical and between two divergencies, black holes solutions does not exists. The only physical cases are small black holes (between root and smaller divergency of the heat capacity) and large black holes (after larger divergency of the heat capacity). It is worthwhile to mention that for the case of $P = P_c$, isothermal compressibility coefficient is positive valued with one divergency which marks the phase transition between small/large black holes. For pressures larger than critical pressure, isothermal compressibility coefficient is positive valued without any root and divergency which agrees with results of other methods.

VI. CONFORMAL FIELD THEORY AND ITS MAGNETIC PROPERTIES

A. Magnetization and magnetic susceptibility of boundary theory

The structure of the dyonic black holes admits a constant magnetic field in dual theory of conformal field theory on the boundary. This constant magnetic field is due to the presence of a magnetic charge on the bulk. It is a matter of calculation to show that the magnetic field is

$$B = \frac{q_M}{l^2}. \quad (69)$$

Considering this magnetic field, it is possible to introduce the corresponding conjugating quantity which is the magnetization. Thermodynamically speaking, different phases living on the boundary of the solutions could be recognized by this quantity. Using the definition of the internal energy (23), one can find magnetization for these black holes as

$$M = - \left(\frac{\partial H}{\partial B} \right) = - \frac{l^2 q_M}{r_+}, \quad (70)$$

which shows that generalization to massive gravity has no direct effect on magnetization. In addition, since b , q_M and r_+ are positive values, magnetic field and magnetization have opposite sign. Now, by using the obtained internal energy (23) and temperature (17) with the magnetic field (69) and magnetization (70), one can rewrite internal energy and temperature in following forms, respectively,

$$H = \frac{B^2 l^8 m^2 c c_1}{4M^2} - \frac{B^3 l^{10}}{2M^3} - \frac{(k + m^2 c^2 c_2 + \Phi_E^2) B l^4}{2M} - \frac{BM}{2}, \quad (71)$$

$$T = \frac{m^2 c c_1}{4\pi} - \frac{(k + m^2 c^2 c_2 - \Phi_E^2) M}{4\pi B l^4} - \frac{3B l^2}{4\pi M} + \frac{M^3}{4\pi B l^8 \pi}. \quad (72)$$

Remembering that phase transition points are marked as extrema of temperature, we obtain the magnetization at the extrema of temperature as

$$M_{Extremum-T} = \frac{l^2 \sqrt{6}}{6} \sqrt{m^2 c^2 c_2 - \Phi_E^2 + k \pm \sqrt{(k + m^2 c^2 c_2 - \Phi_E^2 + 6Bl) (k + m^2 c^2 c_2 - \Phi_E^2 - 6Bl)}}. \quad (73)$$

Evidently, depending on the choices of different parameters, the temperature may be categorized under one the following cases:

I) Absence of extremum. This case happens if the following conditions are not satisfied, simultaneously,

$$(k + m^2 c^2 c_2 - \Phi_E^2 + 6Bl) (k + m^2 c^2 c_2 - \Phi_E^2 - 6Bl) > 0,$$

$$m^2 c^2 c_2 - \Phi_E^2 + k \pm \sqrt{(k + m^2 c^2 c_2 - \Phi_E^2 + 6Bl) (k + m^2 c^2 c_2 - \Phi_E^2 - 6Bl)} > 0.$$

II) Existence of only one extremum which takes place if

$$(k + m^2 c^2 c_2 - \Phi_E^2 + 6Bl) (k + m^2 c^2 c_2 - \Phi_E^2 - 6Bl) = 0$$

III) The presence of two extrema which happens if the mentioned conditions of first case are satisfied.

The existence of magnetic field and magnetization provides the possibility of studying magnetic properties of the solutions. Hereafter, we will focus on diamagnetic and paramagnetic behaviors of the solutions. In ordinary materials, diamagnetic behavior is due to quantized orbital motion of the electrons in the presence of an external magnetic field. On the other hand, paramagnetism originates from alignment of the spin of electrons parallel to external magnetic field. Depending on the dominance of either these two behaviors, materials could be categorized into diamagnetic and paramagnetic ones. The magnetic property which enables one to determine diamagnetic and paramagnetic nature of the material is magnetic susceptibility, χ . The positivity of the susceptibility, $\chi > 0$, indicates that system is diamagnetic while, the opposite ($\chi < 0$) is valid for paramagnetic systems. The susceptibility is defined as

$$\chi = \left(\frac{\partial M}{\partial B} \right), \quad (74)$$

in which, for these black holes, we can find

$$\chi = \frac{\left(\frac{\partial T}{\partial B} \right)}{\left(\frac{\partial T}{\partial M} \right)} = - \frac{M}{B} \frac{(m^2 c^2 c_2 - \Phi_E^2 + k) M^2 l^4 - M^4 - 3 B^2 l^{10}}{(m^2 c^2 c_2 - \Phi_E^2 + k) M^2 l^4 - 3 M^4 - 3 B^2 l^{10}}. \quad (75)$$

If following condition is satisfied

$$0 < (m^2 c^2 c_2 - \Phi_E^2 + k) M^2 l^4 - M^4 - 3 B^2 l^{10} < 2 M^4,$$

the susceptibility will be positive valued and system has diamagnetic behavior, while the opposite is observed for paramagnetic behavior. The roots of susceptibility are obtained in following forms

$$M_{root-\chi} = \frac{l^2 \sqrt{2}}{2} \sqrt{m^2 c^2 c_2 - \Phi_E^2 + k \pm \sqrt{m^2 c^2 c_2 (2k + m^2 c^2 c_2 - 2\Phi_E^2) + \Phi_E^4 + k(k - 2\Phi_E^2) - 12B^2 l^2}}, \quad (76)$$

which points to the following cases:

I) No root exists for the susceptibility. This happens if the following conditions are not satisfied, simultaneously,

$$m^2 c^2 c_2 (2k + m^2 c^2 c_2 - 2\Phi_E^2) + \Phi_E^4 + k(k - 2\Phi_E^2) - 12B^2 l^2 > 0,$$

$$m^2 c^2 c_2 - \Phi_E^2 + k \pm \sqrt{m^2 c^2 c_2 (2k + m^2 c^2 c_2 - 2\Phi_E^2) + \Phi_E^4 + k(k - 2\Phi_E^2) - 12B^2 l^2} > 0.$$

II) Only one root exists which will happen if

$$m^2 c^2 c_2 (2k + m^2 c^2 c_2 - 2\Phi_E^2) + \Phi_E^4 + k(k - 2\Phi_E^2) - 12B^2 l^2 = 0.$$

III) Two roots exists if conditions for the first case are satisfied. The roots usually determines the places where the sign of the susceptibility switches. The phase transition between different phases are marked by divergencies that may exist in the susceptibility. It is a matter of calculation to show that divergencies of the susceptibility are obtained as

$$M_{\infty-\chi} = \frac{l^2 \sqrt{6}}{6} \sqrt{m^2 c^2 c_2 - \Phi_E^2 + k \pm \sqrt{(k + m^2 c^2 c_2 - \Phi_E^2 + 6Bl)(k + m^2 c^2 c_2 - \Phi_E^2 - 6Bl)}}. \quad (77)$$

The obtained divergencies (phase transition) are identical to extrema that were extracted for the temperature (73). This shows that phase transition point in boundary theory are extrema that are observed in the temperature. Therefore, depending on satisfaction of conditions that were pointed out for the temperature, the boundary theory is divided into one of the following cases: I) Absence of phase transition and smooth behavior for the susceptibility. II) Existence of only one phase transition point. III) Existence of two phase transition points for the boundary theory.

B. T vs M and χ vs M diagrams and diamagnetic/paramagnetic behaviors

In this section, we will employ the obtained relations in the previous section to plot $T - M$ and $\chi - M$ diagrams (Figs. 14–17) for studying the diamagnetic and paramagnetic behavior of the solutions.

Fig. 14 is provided as an example of the massless case. The massless case was studied in an interesting paper (we refer the reader to Ref. [143]). We just point out that for large (small) values of magnetic field the phase transition

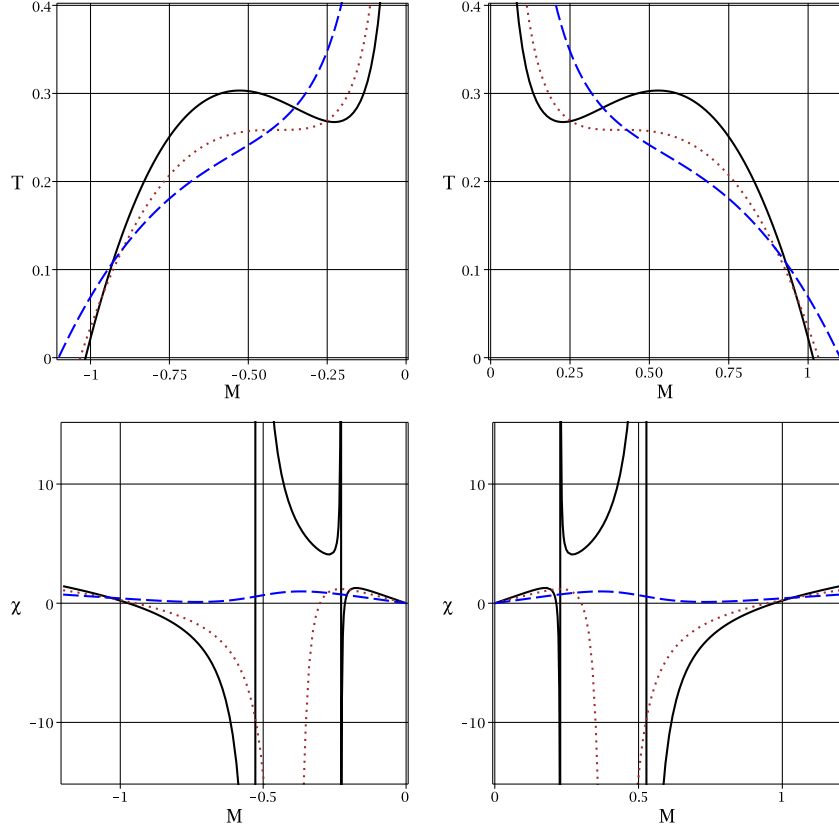


FIG. 14: T (up panels) and χ (down panels) versus M diagrams for $m = 0$, $\Phi_E = 0.1$, $k = 1$ and $b = 1$; **Left panels:** $B = 0.12$ (continuous line), $B = 0.165$ (dashed line) and $B = 0.3$ (dashed-dotted line). **Right panels:** $B = -0.12$ (continuous line), $B = -0.165$ (dashed line) and $B = -0.3$ (dashed-dotted line).

points are eliminated and only paramagnetic phase exists for the boundary theory. Here, we only focus on the effects of massive gravity and topological structure of the solutions.

The first important effect of massive gravity is the existence of phase transitions and roots for non-spherical boundary solutions. Taking a closer look at the obtained roots (76) and divergencies (77) for the susceptibility, one can confirm that in the absence of massive gravity, no root and divergency exists for the susceptibility in non-spherical cases. This indicates that the sign of susceptibility for non-spherical cases remains fixed and only one phase of diamagnetic/paramagnetic exists. But generalization to massive gravity provides the possibility of existence of root and divergency for the susceptibility in non-spherical cases. This leads to the presence of different diamagnetic and paramagnetic behaviors for spherical and non-spherical boundary solutions (see dashed and dashed-dotted lines in Figs. 15-17 in which dashed line is for the existence of only one phase transition while dashed-dotted lines is related to the cases of existence of two phase transition points).

Since B , could be positive or negative, we have plotted two sets of panels in Figs. 15-17 and investigated the effects of the topological factor on the magnetic behavior of the solutions for both branches. Studying dashed lines for Figs. 15-17 shows that divergency is an increasing (decreasing) function of the topological factor. In other words, for the hyperbolic case, obtained divergency is located at larger (smaller) magnetization comparing to horizon flat and spherical cases. One can conclude that phase transition takes place at smaller (larger) magnetization in spherical solutions while such transition happens at larger (smaller) magnetization. This emphasizes the role of the topological structure of the boundary theory.

Generally, the effects of the graviton mass should be separated into four groups which are marked with m_* and m_c . For gravitons lighter than m_* , $0 \leq m < m_*$, for hyperbolic and flat cases (Figs. 15 and 16, respectively), the susceptibility is positive valued and only paramagnetic behavior exists. Increasing mass of the graviton to reach $m_* < m < m_c$ leads to the existence of two crossovers between paramagnetic and diamagnetic phases for non-spherical cases. Evidently, the small and large boundary cases have paramagnetic behavior while the medium solutions are diamagnetic. Therefore, here, we have three phases where small and large ones have paramagnetic behavior whereas the medium phase has diamagnetic properties. The smaller phase of the boundary theory corresponds to the large

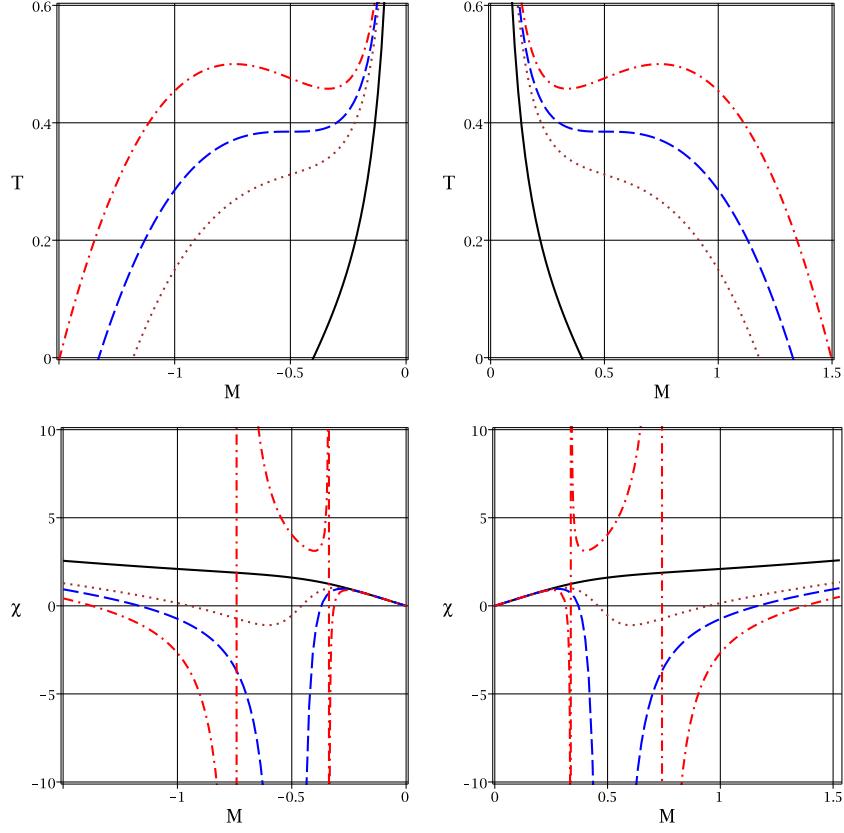


FIG. 15: T (up panels) and χ (down panels) versus M diagrams for $c = c_1 = 2$, $c_2 = 3$, $\Phi_E = 0.1$, $b = 1$ and $k = -1$; $m = 0$ (continuous line), $m = 0.42$ (dotted line), $m = 0.4573474245$ (dashed line) and $m = 0.5$ (dashed-dotted line). **Left panels:** $B = 0.25$; **Right panels:** $B = -0.25$.

black holes while vice versa could be said about the larger phase of the boundary theory. For the spherical case of considered parameters without massive term, the crossovers are observed and single phase is not seen.

For the case $m = m_c$ two crossovers between paramagnetic and diamagnetic are observed with a phase transition located at the diamagnetic region. The crossovers are marked as roots for the susceptibility while the phase transition could be recognized by its divergency. Here two (before smaller root and after larger roots of the susceptibility) solutions have paramagnetic behavior while the intermediate diamagnetic solutions are located between these two roots. Interestingly, the phase transition takes place at the diamagnetic region and it is between two diamagnetic phases. The phase transition here is matched with an extremum in temperature diagrams. For this case, we have two phases of paramagnetism and two phases of diamagnetism.

Finally, for $m_c < m$, the susceptibility acquires two divergencies and two roots. Therefore, here, we have four points which are smaller root ($M_{smallr-root}$), smaller divergency ($M_{smallr-\infty}$), larger divergency ($M_{larger-\infty}$) and larger root ($M_{larger-root}$). These points follow the inequality $M_{smallr-root} < M_{smallr-\infty} < M_{larger-\infty} < M_{larger-root}$. As it is clear, these four points provide five different phases.

For $M < M_{smallr-root}$ and $M_{larger-root} < M$, the susceptibility is positive valued which indicates that paramagnetic phases exist in these two regions. On the other hand, in the cases of $M_{smallr-root} < M < M_{smallr-\infty}$ and $M_{larger-\infty} < M < M_{larger-root}$, the susceptibility is negative which shows that the solutions in these cases have diamagnetic behavior. Interestingly, between two divergencies, we have positive susceptibility which presents a paramagnetic phase. It is worthwhile to mention that both divergencies in the susceptibility are matched with two extrema in the temperature. Remembering the results of previous sections regarding the regions of thermal stability, one can conclude that the region of paramagnetic solutions which is between two divergencies is thermally unstable. Here, when the boundary theory reaches smaller divergency, it jumps to the larger divergency. Therefore, the system never experiences this specific region of the paramagnetism. This phase transition between two different values of magnetization also indicates that specific values of magnetization are not experienced by the boundary theory.

We therefore see that the variation of massive parameter introduces new phase transitions and different phases of diamagnetic/paramagnetic into the phase space of the boundary theory. This shows that depending on the graviton

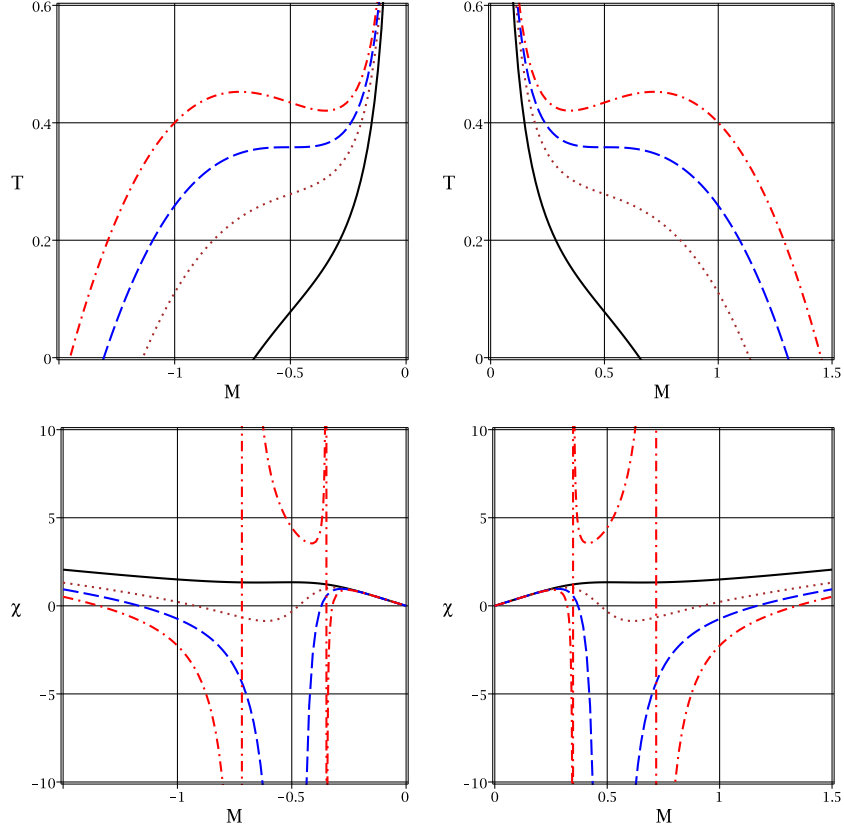


FIG. 16: T (up panels) and χ (down panels) versus M diagrams for $c = c_1 = 2$, $c_2 = 3$, $\Phi_E = 0.1$, $b = 1$ and $k = 0$; $m = 0$ (continuous line), $m = 0.3$ (dotted line), $m = 0.3547299442$ (dashed line) and $m = 0.4$ (dashed-dotted line). **Left panels:** $B = 0.25$; **Right panels:** $B = -0.25$.

mass, the phase structure of the boundary theory might be modified and new phenomena could happen.

Another interesting result appearing from plotted diagrams is that phase transitions of the susceptibility match with extrema of the temperature. In previous sections, we showed that extrema of the temperature, divergencies of the heat capacity, extrema of the free energy and the critical points of van der Waals diagrams coincide with each other. Combining the results of these two sections with each other, one can conclude that the van der Waals like phase transitions of the black holes, divergencies of the heat capacity of black holes and the phase transitions of the boundary theory coincide with each other. Therefore, studying heat capacity of black holes or their van der Waals like phase transitions enables one to make statements regarding phase transition of the boundary theory and these phase transitions are connected.

C. High temperature limit

Our final study for this section concerns the high temperature limit. For the high temperature limit, we can regard the dominant terms of T as

$$T \approx \frac{m^2 c c_1}{4\pi} - \frac{3Bl^2}{4\pi M}. \quad (78)$$

The obtained relation contains massive term which is the correction and the effect of generalization to massive gravity. Here, the massive term is not coupled with magnetic field and magnetization, which indicates that it plays the role of a constant. As for the susceptibility, we see that the high energy limit leads to

$$\chi \approx -\frac{M}{B}, \quad (79)$$

in which by using Eq. (78), one can find

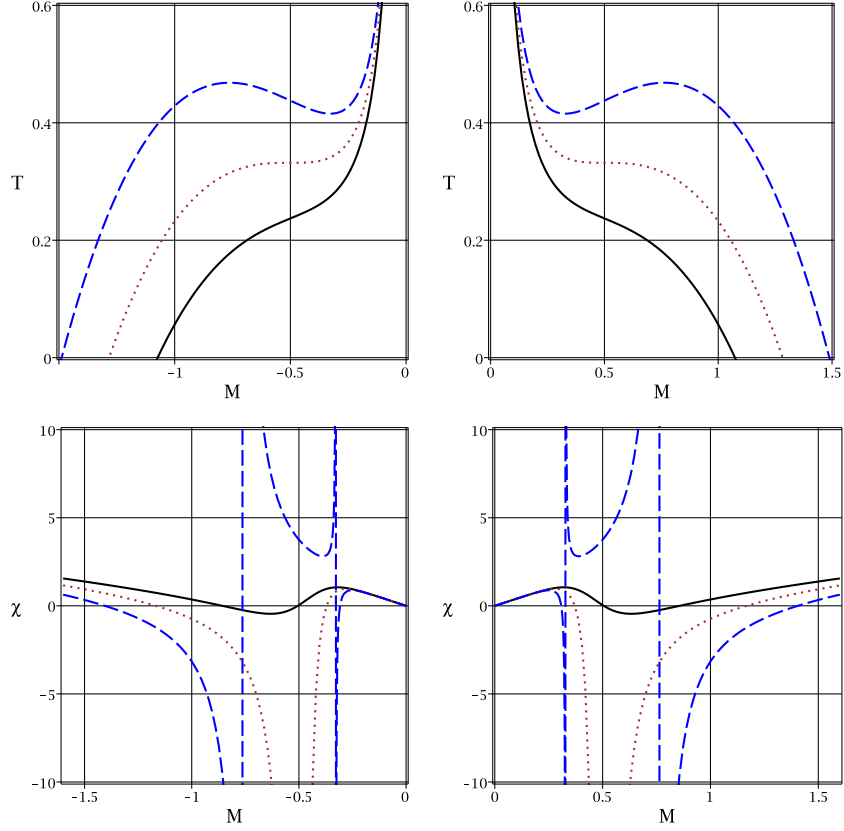


FIG. 17: T (up panels) and χ (down panels) versus M diagrams for $c = c_1 = 2$, $c_2 = 3$, $\Phi_E = 0.1$, $b = 1$ and $k = 1$; $m = 0$ (continuous line), $m = 0.2061552812$ (dashed line) and $m = 0.3$ (dashed-dotted line). **Left panels:** $B = 0.25$; **Right panels:** $B = -0.25$.

$$\chi \approx \frac{3l^2}{4\pi T - m^2 c c_1} \approx \frac{3l^2}{4\pi T} + \frac{3l^2 m^2 c c_1}{16\pi^2 T^2} + O(T^{-3}). \quad (80)$$

Here, we see the Curie constant which is given by $(\frac{4\pi}{3b^2})^{-1}$ and a correction a correction of Curie law which is due to generalization to massive gravity for high temperature limit of the susceptibility.

VII. CLOSING REMARKS

This paper included a thermodynamical study of charged dyonic black holes in the presence of massive gravity and holographical aspects of its dual boundary CFT . Thermodynamical quantities were extracted and it was shown that existence of the massive gravity term modifies conserved and thermodynamical quantities of the black holes. These modifications introduce new phenomena with the most important ones being: existence of remnant for the temperature in evaporation of black holes, van der Waals behavior and phase transition for non-spherical black holes.

Thermal stability and conditions for having physical solutions were investigated. In addition, the free energy and its properties were discussed. The concept of extended phase space was also employed to extract phase transition points and plot the van der Waals like diagrams. The limiting cases were also studied and it was shown that existence of critical behavior is magnetic charge dependent. It was also pointed out that generalization to massive gravity leads to the presence of van der Waals like behavior for non-spherical black holes. This essentially resulted into the existence of second order phase transitions in the boundary theory with non-spherical horizons (hyperbolic and planar) as well. Furthermore, an alternative method was employed to extract critical points which presented themselves as maxima in the phase diagrams. More importantly, it was shown that the critical points that were extracted through different methods were consistent. In addition, a comparative study regarding thermal stability and van der Waals like phase transition was done and thermodynamical behavior of the black holes in unstable regions was discussed.

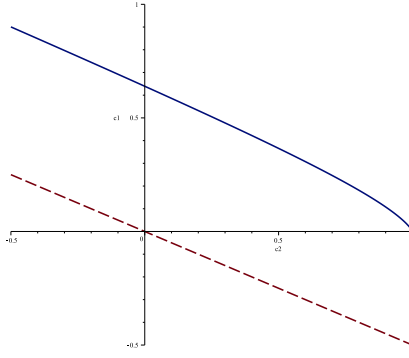


FIG. 18: c_1 versus c_2 for $r_h = 2$, $c = m = \Phi_E = 1$ and $q_M = P = k = 0$.

solid diagram: $c_1 = \frac{1}{2}(c_2 - 1) \left(-1 - \text{LambertW}\left(\frac{e^{-1}}{1-c_2}\right) \right)$ and **dashed diagram:** $c_1 = -\frac{c_2}{2}$.

Next, the properties of the boundary *CFT* dual to the bulk theory were investigated. It was shown that depending on the choices of different allowed parameters (see appendix), the boundary theory may have; only one paramagnetic phase, two paramagnetic and one diamagnetic phases, two paramagnetic and two diamagnetic phases with a phase transition between the two diamagnetic phases and finally, two paramagnetic and two diamagnetic phases with two phase transitions and one thermally unstable paramagnetic phase.

Finally, it was pointed out that the high temperature limit of holographical aspect is free of massive term up to first dominant term. However, the graviton mass effects will appear as the second dominant term of high temperature limit. The correction terms were shown to be necessary in the expressions for temperature, the susceptibility of boundary theory and the Curie law.

In this paper, we also investigated linear electrodynamics in the context of massive gravity. It will be interesting to generalize our results to the cases of nonlinear electrodynamics and higher derivative gravity. In addition, it is worthwhile to study new massive gravity in this regards. The massive gravity considered in this paper enjoys the Lorentz violating property. The existence of Lorentz violating property provides the possibility of constructing other consistent massive gravity theories which could be expressed in Stueckelberg form. Several of these theories were introduced and employed in the context of holography [157–160]. The thermodynamical quantities and behavior that were reported for obtained black holes in this paper will be modified if other generic theories of the massive gravity are employed. It would be interesting to see how the behaviors reported in this paper could be modified if other theories of the massive gravity are employed. In addition, we have investigated thermodynamic stability of the solutions in this work. It is interesting to study dynamical stability and anti-evaporation of such solutions [161–163] in a separate work.

Appendix

Here, we are going to study the regime where the graviton mass is positive [58, 164]. Following the method of Ref. [58], one finds two relations for the massive parameters, which could be employed to find the stability (positive mass of gravitons) condition in the parameter space. One of the mentioned relations comes from identification of entropy density calculated from the finite Euclidean action and what we obtain from the area law. Such identification leads to

$$\sum_{R=R_0} \frac{R^3 \ln(r_h - R)}{3m^2 c c_1 R^2 + 2m^2 c^2 c_2 R + 32\pi P R^3 - 2\Phi_E^2 R + 2kR} = 0, \quad (81)$$

where R_0 is the root of the following equation

$$8\pi P R_0^4 + m^2 c c_1 R_0^4 + (m^2 c^2 c_2 - \Phi_E^2 + k) R_0^4 - q_M^2 = 0.$$

The other relation can be obtained from maximizing the chemical potential by setting $q_E = q_M = 0$ in the vanishing temperature. After straightforward calculations, we find

$$c_2 = -\frac{r_h}{c} c_1 - \frac{8\pi P r_h^2}{m^2 c^2} - \frac{k}{m^2 c^2}. \quad (82)$$

Because of the existence of cosmological constant (pressure), in the first relation (81), it is not possible to obtain the required relation analytically, therefore we have employed numerical method. For more clarity, we plot Fig. 18 as

an example of parameter space. It is worth mentioning that the solid line is related to Eq. (81), while dashed line is plotted based on Eq. (82). As it mentioned in Ref. [58], the region between these lines is allowed parameter space, while other zones are forbidden.

Acknowledgments

We thank the anonymous reviewers for their careful reading of our manuscript and their many insightful comments and suggestions. We also thank both Shiraz University and Shahid Beheshti University Research Councils. This work has been supported financially by the Research Institute for Astronomy and Astrophysics of Maragha, Iran.

-
- [1] G. T. Horowitz, ‘The Dark Side of String Theory: Black Holes and Black Strings,’ UCSBTH-92-32 (1992).
 - [2] G. T. Horowitz, ‘What is the True Description of Charged Black Hole,’ UCSBTH-92-52 (1992).
 - [3] J. A. Harvey and J. A. Strominger, ‘Quantum Aspects of Black Holes,’ EFI-92-41 (1992).
 - [4] A. O. Barut, Phys. Rev. D 3, 1747 (1971).
 - [5] A. H. Taub, Ann. Math. 53, 472 (1951).
 - [6] E. T. Newman, L. Tamburino and T. Unti, J. Math. Phys. 4, 915 (1963).
 - [7] C. W. Misner, J. Math. Phys. 4, 924 (1963).
 - [8] C. W. Misner and A. H. Taub, Sov. Phys. JETP 28, 122 (1969).
 - [9] M. H. Dehghani and S. H. Hendi, Phys. Rev. D 73, 084021 (2006).
 - [10] S. H. Hendi and M. H. Dehghani, Phys. Lett. B 666, 116 (2008).
 - [11] M. Damianski and E. T. Newman, Bull. Acad. Pol. Sci. 14, 653 (1966).
 - [12] J. S. Dowker, Gen. Rel. Grav. 5, 603 (1974).
 - [13] G. J. Cheng, R. R. Hsu and W. F. Lin, J. Math. Phys. 35, 4839 (1994).
 - [14] D. A. Lowe and A. Strominger, Phys. Rev. Lett. 73, 1468 (1994).
 - [15] S. Mignemi, Phys. Rev. D 51, 934 (1995).
 - [16] A. A. Tseytlin, Mod. Phys. Lett. A 11, 689 (1996).
 - [17] D. P. Jatkar, S. Mukherji and S. Panda, Nucl. Phys. B 484, 223 (1997).
 - [18] Y. Brihaye, B. Hartmann and J. Kunz, Phys. Lett. B 441, 77 (1998).
 - [19] P. K. Tripathy, Phys. Lett. B 463, 1 (1999).
 - [20] A. H. Chamseddine and W. A. Sabra, Phys. Lett. B 485, 301 (2000).
 - [21] G. L. Cardoso, B. de Wit, J. Käppeli and T. Mohaupt, JHEP 12, 075 (2004).
 - [22] C. M. Chen, D. V. Gal’tsov and D. G. Orlov, Phys. Rev. D 78, 104013 (2008).
 - [23] M. M. Caldarelli, O. J. C. Dias and D. Klemm, JHEP 03, 025 (2009).
 - [24] C. M. Chen, Y. M. Huang, J. R. Sun, M. F. Wu and S. J. Zou, Phys. Rev. D 82, 066003 (2010).
 - [25] B. C. Nolan and E. Winstanley, Class. Quant. Grav. 29, 235024 (2012).
 - [26] H. Lu, Y. Pang and C. N. Pope, JHEP 11, 033 (2013).
 - [27] D. D. K. Chow and G. Compère, Phys. Rev. D 89, 065003 (2014).
 - [28] R. G. Cai and R. Q. Yang, Phys. Rev. D 90, 081901 (2014).
 - [29] S. Q. Wu and S. Li, Phys. Lett. B 746, 276 (2015).
 - [30] J. E. Baxter, J. Math. Phys. 57, 022505 (2016).
 - [31] B. L. Shepherd and E. Winstanley, Phys. Rev. D 93, 064064 (2016).
 - [32] M. Cárdenas, O. Fuentealba and J. Matulich, JHEP 05, 001 (2016).
 - [33] S. Li, H. Lu and H. Wei, JHEP 07, 004 (2016).
 - [34] S. N. Gupta, Phys. Rev. 96, 1683 (1954).
 - [35] S. Weinberg, Phys. Rev. 138, B988 (1965).
 - [36] S. Deser, Gen. Rel. Grav. 1, 9 (1970).
 - [37] D. G. Boulware and S. Deser, Ann. Phys. 89, 193 (1975).
 - [38] M. Fierz and W. Pauli, Proc. Roy. Soc. Lond. A 173, 211 (1939).
 - [39] H. van Dam and M. J. G. Veltman, Nucl. Phys. B 22, 397 (1970).
 - [40] V. I. Zakharov, JETP Lett. 12, 312 (1970).
 - [41] S. Deser and A. Waldron, Phys. Rev. D 89, 027503 (2013).
 - [42] A. I. Vainshtein, Phys. Lett. B 39, 393 (1972).
 - [43] D. G. Boulware and S. Deser, Phys. Rev. D 6, 3368 (1972).
 - [44] G. R. Dvali and G. Gabadadze, Phys. Rev. D 63, 065007 (2001).
 - [45] G. R. Dvali, G. Gabadadze and M. Porrati, Phys. Lett. B 485, 208 (2000).
 - [46] G. R. Dvali, G. Gabadadze and M. Porrati, Phys. Lett. B 484, 112 (2000).
 - [47] E. A. Bergshoeff, O. Hohm and P. K. Townsend, Phys. Rev. Lett. 102, 201301 (2009).
 - [48] S. F. Hassan and R. A. Rosen, JHEP 02, 126 (2012).

- [49] C. de Rham, G. Gabadadze and A. J. Tolley, *Phys. Rev. Lett.* 106, 231101 (2011).
- [50] C. de Rham, G. Gabadadze and A. J. Tolley, *Phys. Lett. B* 711, 190 (2012).
- [51] K. Hinterbichler, *Rev. Mod. Phys.* 84, 671 (2012).
- [52] S. F. Hassan, A. Schmidt-May, M. von Strauss, *Phys. Lett. B* 715, 335 (2012).
- [53] S. F. Hassan and R. A. Rosen, *Phys. Rev. Lett.* 108, 041101 (2012).
- [54] S. F. Hassan, R. A. Rosen and A. Schmidt-May, *JHEP* 02, 026 (2012).
- [55] C. de Rham, *Living Rev. Relativ.* 17, 7 (2014).
- [56] I. Arraut, [arXiv:1503.02150].
- [57] I. Arraut, *Europhys. Lett.* 109, 10002 (2015).
- [58] D. Vegh, [arXiv:1301.0537].
- [59] S. H. Hendi, B. Eslam Panah and S. Panahiyan, *Class. Quant. Grav.* 33, 235007 (2016).
- [60] S. H. Hendi, B. Eslam Panah and S. Panahiyan, *Phys. Lett. B* 769, 191 (2017).
- [61] S. H. Hendi, B. Eslam Panah and S. Panahiyan, *JHEP* 11, 157 (2015).
- [62] S. H. Hendi, S. Panahiyan and B. Eslam Panah, *JHEP* 01, 129 (2016).
- [63] S. H. Hendi, B. Eslam Panah and S. Panahiyan, *JHEP* 05, 029 (2016).
- [64] S. H. Hendi, G. H. Bordbar, B. Eslam Panah and S. Panahiyan, *JCAP* 07, 004 (2017).
- [65] G. D'Amico, C. de Rham, S. Dubovsky, G. Gabadadze, D. Pirtskhalava and A. J. Tolley, *Phys. Rev. D* 84, 124046 (2011).
- [66] A. E. Gumrukcuoglu, C. Lin and S. Mukohyama, *JCAP* 11, 030 (2011).
- [67] N. Khosravi, G. Niz, K. Koyama and G. Tasinat, *JCAP* 08, 044 (2013).
- [68] A. De Felice, A. E. Gumrukcuoglu and S. Mukohyama, *Phys. Rev. Lett.* 109, 171101 (2012).
- [69] G. Dvali, G. Gabadadze and M. Shifman, *Phys. Rev. D* 67, 044020 (2003).
- [70] G. Dvali, S. Hofmann and J. Khoury, *Phys. Rev. D* 76, 084006 (2007).
- [71] C. Deffayet, *Phys. Lett. B* 502, 199 (2001).
- [72] C. Deffayet, G. Dvali and G. Gabadadze, *Phys. Rev. D* 65, 044023 (2002).
- [73] P. Gratia, W. Hu and M. Wyman, *Phys. Rev. D* 86, 061504 (2012).
- [74] T. Kobayashi, M. Siino, M. Yamaguchi and D. Yoshida, *Phys. Rev. D* 86, 061505 (2012).
- [75] J. D. Bekenstein, *Phys. Rev. D* 7, 2333 (1973).
- [76] S. W. Hawking, *Phys. Rev. Lett.* 26, 1344 (1971).
- [77] J. M. Bardeen, B. Carter and S. W. Hawking, *Commun. Math. Phys.* 31, 161 (1973).
- [78] B. P. Dolan, *Class. Quant. Grav.* 28, 125020 (2011).
- [79] B. P. Dolan, *Class. Quant. Grav.* 28, 235017 (2011).
- [80] D. Grumiller, R. McNees and J. Salzer, *Phys. Rev. D* 90, 044032 (2014).
- [81] S. H. Hendi, S. Panahiyan and R. Mamasani, *Gen. Rel. Grav.* 47, 91 (2015).
- [82] B. P. Dolan, *JHEP* 10, 179 (2014).
- [83] D. Kastor, S. Ray and J. Traschen, *JHEP* 11, 120 (2014).
- [84] A. Karch and B. Robinson, *JHEP* 12, 073 (2015).
- [85] E. Caceres, P. H. Nguyen and J. F. Pedraza, *JHEP* 09, 184 (2015).
- [86] X. X. Zeng and L. F. Li, *Phys. Lett. B* 764, 100 (2017).
- [87] Z. Y. Nie and H. Zeng, *JHEP* 10, 047 (2015).
- [88] B. P. Dolan, *Entropy* 18, 169 (2016).
- [89] D. Kubiznak and R. B. Mann, *JHEP* 07, 033 (2012).
- [90] S. Gunasekaran, R. B. Mann and D. Kubiznak, *JHEP* 11, 110 (2012).
- [91] N. Altamirano, D. Kubiznak and R. B. Mann, *Phys. Rev. D* 88, 101502 (2013).
- [92] A. M. Frassino, D. Kubiznak, R. B. Mann and F. Simovic, *JHEP* 09, 080 (2014).
- [93] R. A. Hennigar and R. B. Mann, *Entropy* 17, 8056 (2015).
- [94] N. Altamirano, D. Kubiznak, R. B. Mann and Z. Sherkatghanad, *Class. Quant. Grav.* 31, 042001 (2014).
- [95] S. W. Wei and Y. X. Liu, *Phys. Rev. D* 90, 044057 (2014).
- [96] R. A. Hennigar, W. G. Brenna and R. B. Mann, *JHEP* 07, 077 (2015).
- [97] C. V. Johnson, *Class. Quant. Grav.* 31, 205002 (2014).
- [98] A. Belhaj, M. Chabab, H. El Moumni, K. Masmar, M. B. Sedra and A. Segui, *JHEP* 05, 149 (2015).
- [99] M. R. Setare and H. Adami, *Gen. Rel. Grav.* 47, 133 (2015).
- [100] C. V. Johnson, [arXiv:1511.08782].
- [101] C. V. Johnson, *Class. Quant. Grav.* 33, 135001 (2016).
- [102] C. Bhamidipati and P. K. Yerra, *Eur. Phys. J. C* 77, 534 (2017).
- [103] J. Sadeghi and K. Jafarzade, *Int. J. Mod. Phys. D* 26, 1750138 (2017).
- [104] J. Sadeghi and K. Jafarzade, [arXiv:1504.07744].
- [105] C. V. Johnson, *Entropy* 18, 120 (2016).
- [106] S. H. Hendi and M. H. Vahidinia, *Phys. Rev. D* 88, 084045 (2013).
- [107] E. Spallucci and A. Smailagic, *Phys. Lett. B* 723, 436 (2013).
- [108] J. X. Mo and W. B. Liu, *Phys. Lett. B* 727, 336 (2013).
- [109] M. B. J. Poshteh, B. Mirza and Z. Sherkatghanad, *Phys. Rev. D* 88, 024005 (2013).
- [110] R. G. Cai, L. M. Cao, L. Li and R. Q. Yang, *JHEP* 09, 005 (2013).
- [111] R. Zhao, H. H. Zhao, M. S. Ma and L. C. Zhang, *Eur. Phys. J. C* 73, 2645 (2013).
- [112] J. X. Mo, X. X. Zeng, G. Q. Li, X. Jiang and W. B. Liu, *JHEP* 10, 056 (2013).

- [113] N. Altamirano, D. Kubiznak, R. B. Mann and Z. Sherkatghanad, *Galaxies* 2, 89 (2014).
- [114] D. C. Zou, S. J. Zhang and B. Wang, *Phys. Rev. D* 89, 044002 (2014).
- [115] J. X. Mo and W. B. Liu, *Eur. Phys. J. C* 74, 2836 (2014).
- [116] C. V. Johnson, *Class. Quant. Grav.* 31, 225005 (2014).
- [117] B. P. Dolan, *Fortsch. Phys.* 62, 892 (2014).
- [118] J. X. Mo and W. B. Liu, *Phys. Rev. D* 89, 084057 (2014).
- [119] Y. Liu, D. C. Zou and B. Wang, *JHEP* 09, 179 (2014).
- [120] A. Rajagopal, D. Kubiznak and R. B. Mann, *Phys. Lett. B* 737, 277 (2014).
- [121] H. Xu, W. Xu and L. Zhao, *Eur. Phys. J. C* 74, 3074 (2014).
- [122] M. H. Dehghani, S. Kamrani and A. Sheykhi, *Phys. Rev. D* 90, 104020 (2014).
- [123] W. Xu and L. Zhao, *Phys. Lett. B* 736, 214 (2014).
- [124] B. Mirza and Z. Sherkatghanad, *Phys. Rev. D* 90, 084006 (2014).
- [125] H. H. Zhao, L. C. Zhang, M. S. Ma and R. Zhao, *Phys. Rev. D* 90, 064018 (2014).
- [126] T. Delsate and R. Mann, 02, 070 (2015).
- [127] S. H. Hendi, S. Panahiyan and B. Eslam Panah, *Prog. Theor. Exp. Phys.* 2015, 103E01 (2015).
- [128] S. Q. Lan, J. X. Mo and W. B. Liu, *Eur. Phys. J. C* 75, 419 (2015).
- [129] S. W. Wei and Y. X. Liu, *Phys. Rev. Lett.* 115, 111302 (2015).
- [130] H. H. Zhao, L. C. Zhang, M. S. Ma and R. Zhao, *Class. Quant. Grav.* 32, 145007 (2015).
- [131] M. Zhang, Z. Y. Yang, D. C. Zou, W. Xu and R. H. Yue, *Gen. Rel. Grav.* 47, 14 (2015).
- [132] S. H. Hendi, A. Sheykhi, S. Panahiyan and B. Eslam Panah, *Phys. Rev. D* 92, 064028 (2015).
- [133] J. Xu, L. M. Cao and Y. P. Hu, *Phys. Rev. D* 91, 124033 (2015).
- [134] J. L. Zhang, R. G. Cai and H. Yu, *Phys. Rev. D* 91, 044028 (2015).
- [135] P. Cheng, S. W. Wei and Y. X. Liu, *Phys. Rev. D* 94, 024025 (2016).
- [136] S. H. Hendi, S. Panahiyan and M. Momennia, *Int. J. Mod. Phys. D* 25, 1650063 (2016).
- [137] S. H. Hendi, S. Panahiyan, B. Eslam Panah, M. Faizal and M. Momennia, *Phys. Rev. D* 94, 024028 (2016).
- [138] X. X. Zeng, X. M. Liu and L. F. Li, *Eur. Phys. J. C* 76, 616 (2016).
- [139] D. Hansen, D. Kubiznak and R. B. Mann, [arXiv:1603.05689].
- [140] H. Liu and X. H. Meng, *Mod. Phys. Lett. A* 31, 1650199 (2016).
- [141] D. Kubiznak, R. B. Mann and M. Teo, *Class. Quant. Grav.* 34, 063001 (2017).
- [142] R. G. Cai, Y. P. Hu, Q. Y. Pan and Y. L. Zhang, *Phys. Rev. D* 91, 024032 (2015).
- [143] S. Dutta, A. Jainyand and R. Soniz, *JHEP* 12, 060 (2013).
- [144] M. Baggioli and W. J. Li, *JHEP* 07, 055 (2017).
- [145] W. J. Jiang, H. S. Liu, H. Lu and C.N. Pope, [arXiv:1703.00922].
- [146] S. H. Hendi, R. B. Mann, S. Panahiyan and B. Eslam Panah, *Phys. Rev. D* 95, 021501(R) (2017).
- [147] B. P. Dolan, *JHEP* 10, 149 (2014).
- [148] D. Kastor, S. Ray and J. Traschen, *JHEP* 11, 120 (2014).
- [149] A. Karch and B. Robinson, *JHEP* 12, 073 (2015).
- [150] Z. Y. Nie and H. Zeng, *JHEP* 10, 047 (2015).
- [151] E. Caceres, P. H. Nguyen and J. F. Pedraza, *JHEP* 09, 184 (2015).
- [152] S. H. Hendi, S. Panahiyan and B. Eslam Panah, *Int. J. Mod. Phys. D* 25, 1650010 (2016).
- [153] J. X. Mo and W. B. Liu, *Phys. Rev. D* 89, 084057 (2014).
- [154] B. P. Dolan, *Phys. Rev. D* 84, 127503 (2011).
- [155] B. P. Dolan, *Class. Quant. Grav.* 31, 035022 (2014).
- [156] D. C. Zou, Y. Liu and R. Yue, *Eur. Phys. J. C* 77, 365 (2017).
- [157] T. Andrade and B. Withers, *JHEP* 05, 101 (2014).
- [158] M. Taylor and W. Woodhead, *Eur. Phys. J. C* 74, 3176 (2014).
- [159] M. Baggioli and O. Pujolas, *Phys. Rev. Lett.* 114, 25160 (2015).
- [160] L. Alberte, M. Baggioli, A. Khmelnsky and O. Pujolas, *JHEP* 02, 114 (2016).
- [161] S. Nojiri, S. D. Odintsov and N. Shirai, *JCAP* 05, 020 (2013).
- [162] S. Nojiri, S. D. Odintsov, *Phys. Lett. B* 735, 376 (2014).
- [163] T. Katsuragawa and S. Nojiri, *Phys. Rev. D* 91, 084001 (2015).
- [164] R. A. Davison, *Phys. Rev. D* 88, 086003 (2013).